SANDIA REPORT
SAND2018-9134X
Unlimited Release
Printed August 2018

Permeability and Direct Shear Test Determinations of Barnwell Core in Support of UNESE

Scott Broome, Mathew Ingraham, and Perry Barrow

Prepared by
Sandia National Laboratories
Albuquerque, New Mexico 87185 and Livermore, California 94550

Sandia National Laboratories is a multimission laboratory managed and operated by National Technology and Engineering Solutions of Sandia, LLC, a wholly owned subsidiary of Honeywell International, Inc., for the U.S. Department of Energy's National Nuclear Security Administration under contract DE-NA0003525.

Issued by Sandia National Laboratories, operated for the United States Department of Energy by National Technology and Engineering Solutions of Sandia, LLC.

Available to DOE and DOE contractors from
U.S. Department of Energy
Office of Scientific and Technical Information
P.O. Box 62
Oak Ridge, TN 37831

Telephone: (865) 576-8401
Facsimile: (865) 576-5728
E-Mail: reports@osti.gov
Online ordering: http://www.osti.gov/scitech

Available to the public from
U.S. Department of Commerce
National Technical Information Service
5301 Shawnee Rd
Alexandria, VA 22312

Telephone: (800) 553-6847
Facsimile: (703) 605-6900
E-Mail: orders@ntis.gov
Online order: https://classic.ntis.gov/help/order-methods/

SAND2018-9134
Printed August 2018
Unlimited Release

Permeability and Direct Shear Test Determinations of Barnwell Core in Support of UNESE

Scott Broome, Mathew Ingraham, and Perry Barrow
Geomechanics Department
Sandia National Laboratories
P.O. Box 5800
Albuquerque, NM 87185-0751

Abstract

A critical component of the Underground Nuclear Explosion Signatures Experiment (UNESE) program is a realistic understanding of the post-detonation processes and changes in the environment that produce observable physical and radio-chemical signatures. Rock and fracture properties are essential parameters for any UNESE test bed. In response to the need for accurate modeling scenarios of these observations, an experimental program to determine the permeability and direct shear fracture properties of Barnwell core was developed. Room temperature gas permeability measurements of Barnwell core dried at 50°C yield permeability ranging from 6.24E-02 Darcys to 6.98E-08 Darcys. Friction angles from the direct shear tests vary from 28.1° to 44.4° for residual shear strength and average 47.9° for peak shear strength. Cohesion averaged 3.2 psi and 13.3 psi for residual and peak shear strength values respectively. The work presented herein is the initial determination of an ongoing broader material characterization effort.

ACKNOWLEDGMENTS

The authors would like to thank Steve Bauer and Thomas Dewers for their critical review of this report.

TABLE OF CONTENTS

FIGURES

TABLES

1. INTRODUCTION

A critical component of the Underground Nuclear Explosion Signatures Experiment (UNESE) program is a realistic understanding of the post-detonation processes and changes in the environment that produce observable physical and radio-chemical signatures. As such, knowledge of the pre and post-detonation rock and fracture properties are essential parameters for any UNESE test bed. In response to the need for accurate modeling scenarios of these observations, an experimental program was developed to determine the permeability and direct shear properties of core near site U-20az of the Nevada National Security Site.

Room temperature gas permeability measurements of core dried at 50°C and subjected to confining pressure varying from 500 psi to 2500 psi were completed. Direct shear tests performed on dry samples provided insight into fracture cohesion and friction angle variability between natural fractures and an induced fracture surface created from a preexisting weakness plane. All testing was performed on pre-test core, i.e. rock core collected before the Barnwell underground nuclear explosion (UNE) was conducted at the U-20az site. Future material characterization on rock from the Barnwell site is planned. The future work will include hydrostatic (pore crush), strength properties, and laboratory noble gas migration.

2. TEST SETUP AND METHODS

2.1. Permeability

Permeability measurements were completed on nine samples from a set of core holes close to the UNE hole, U-20az. Samples were sub cored out of the received core; the sub cores were parallel to the original coring direction. Sub coring was performed primarily to have samples of the same diameter for flow area consistency and for consistency within the testing system. A gas permeameter with constant pressure and flow rate was used. The samples were cored and ground parallel to approximately 2 inch diameter and 2 to 3 inches in length. After drying at 50°C for at least 24 hours, the cored and ground samples were weighed and measured assuming right circular cylinder geometry to determine density.

Acoustic compression (longitudinal) and shear wave velocities were measured on all of the permeability samples, along the axis (Axial) and also orthogonal across the diameter (Lateral) (shown in Figure 1). Pulse generator and receiver transducers were attached to the samples at positions diametrically opposed to one another. The generator produced a fast-rising, short duration electrical pulse to the transducer which induced elastic compression and shear waves into the specimen. The frequency of the pulse generator and receiver transducers is 1 MHz. The origin time of the wave was established by recording the electrical pulse on a digital oscilloscope. The analysis consisted of selecting the arrival times of the compression and shear waves, knowing the origin time of the induced pulse, and then calculating velocities as the ratios of the sample length (or diameter) to the respective arrival times.

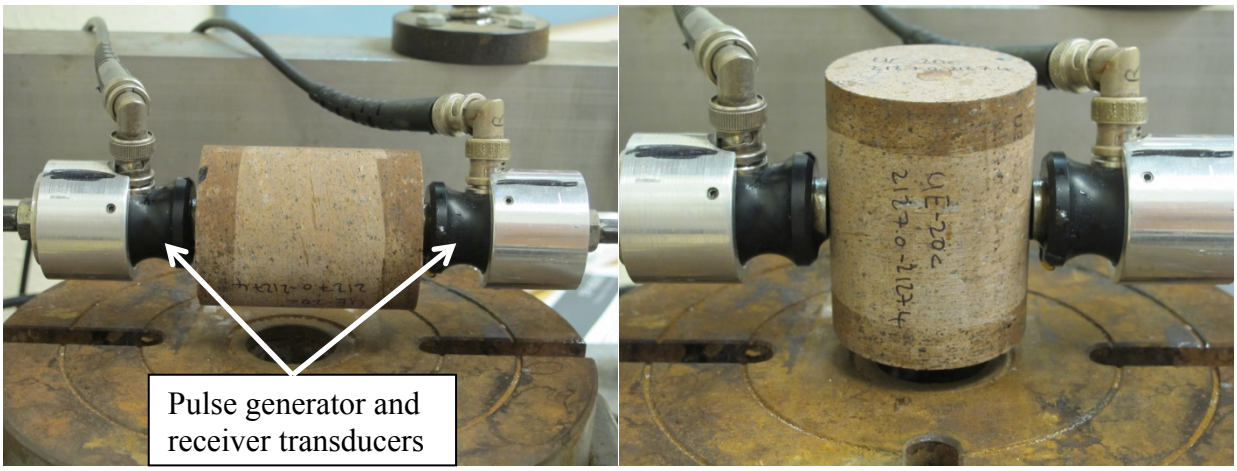

Figure 1. Velocity measurement performed in axial (parallel to core axis) and lateral orientations.

After velocity measurements were recorded, the samples were placed between two metal platens having central ports that permit the permeant (nitrogen or helium) to enter and exit the specimen (Figure 2). Highly-permeable porous felt metal disks are placed in the interface between the platens and specimen to distribute the permeant and permeant pressure across the full cross-section of the specimen. The specimen is jacketed with paint on UV cured polyurethane that is sealed by adhesion to the platens and rock and serves to protect the specimen from hydraulic confining fluid and also to prevent permeant from short-circuiting around the sides of the specimen during testing.

The jacketed specimen/platen assembly was placed inside a pressure vessel (permeameter) and the upstream and downstream ports of the platens were connected to a permeant source and to either a flow meter or helium mass spectrometer (Figure 3, Figure 4). The annulus between the specimen and pressure vessel is filled with Isopar H fluid and pressurized during the test (applying a pressure to the external surface of the specimen). The confining pressure was varied to simulate lithostatic stresses of interest with the highest confining pressure being 2500 psi equating to approximately 2500 feet of depth below ground surface. Confining pressure also assures gas flow goes through the sample and not between the jacket and sample by maintaining the confining pressure higher than the permeant pressure.

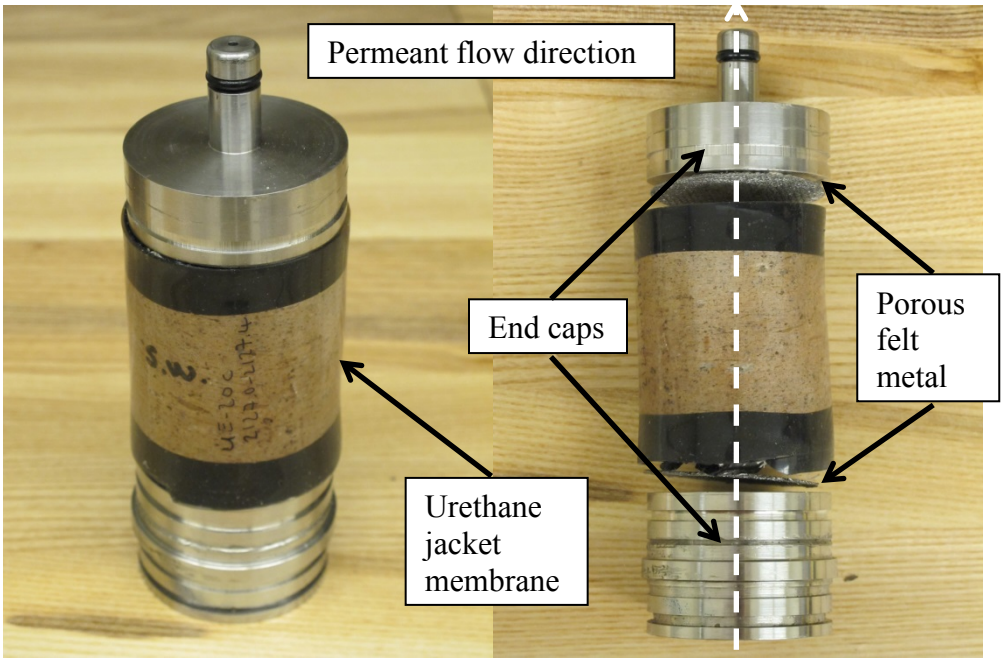

Figure 2. Sample assembly.

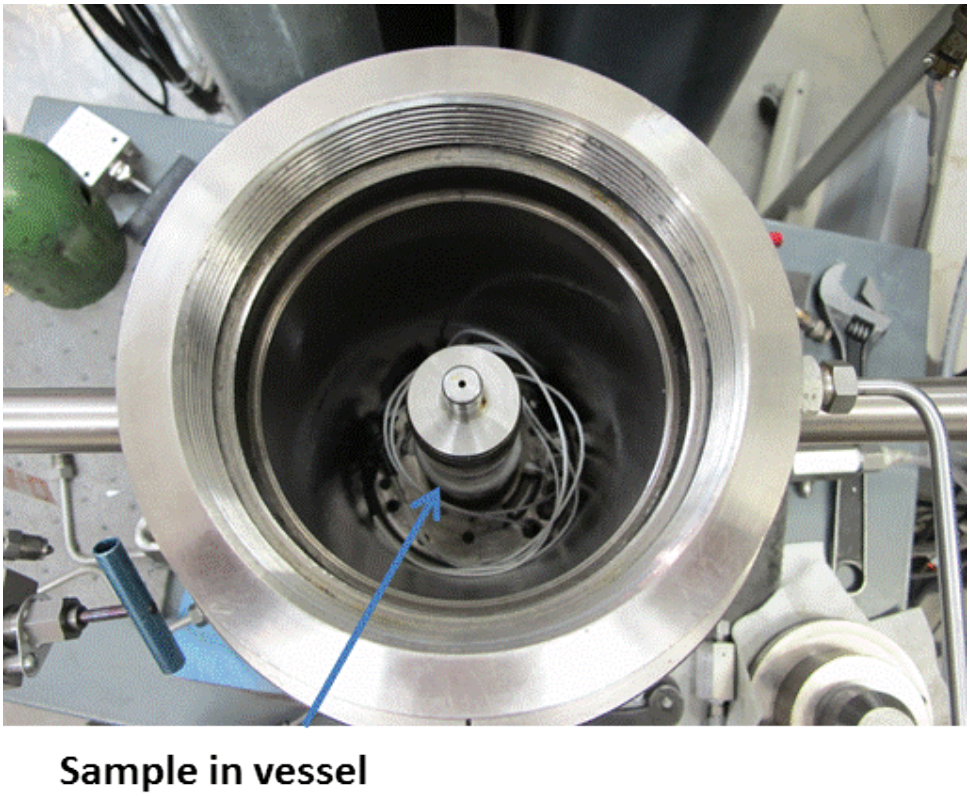

Figure 3. Sample in pressure vessel.

The permeability measurement used a constant head (or pressure) technique with nitrogen or helium as the permeant medium. In this technique, once the confining pressure is slowly raised and stabilized to a constant value, permeant was allowed to enter the upstream side of the specimen at a constant pressure. The pressure difference between the upstream and downstream ends of the sample was minimized. The downstream side of the specimen was either vented to the atmosphere through a flow meter or kept under vacuum when using the helium mass spectrometer. The flow meter and helium mass spectrometer were connected to the data acquisition system and recorded along with confining pressure, upstream pressure and time.

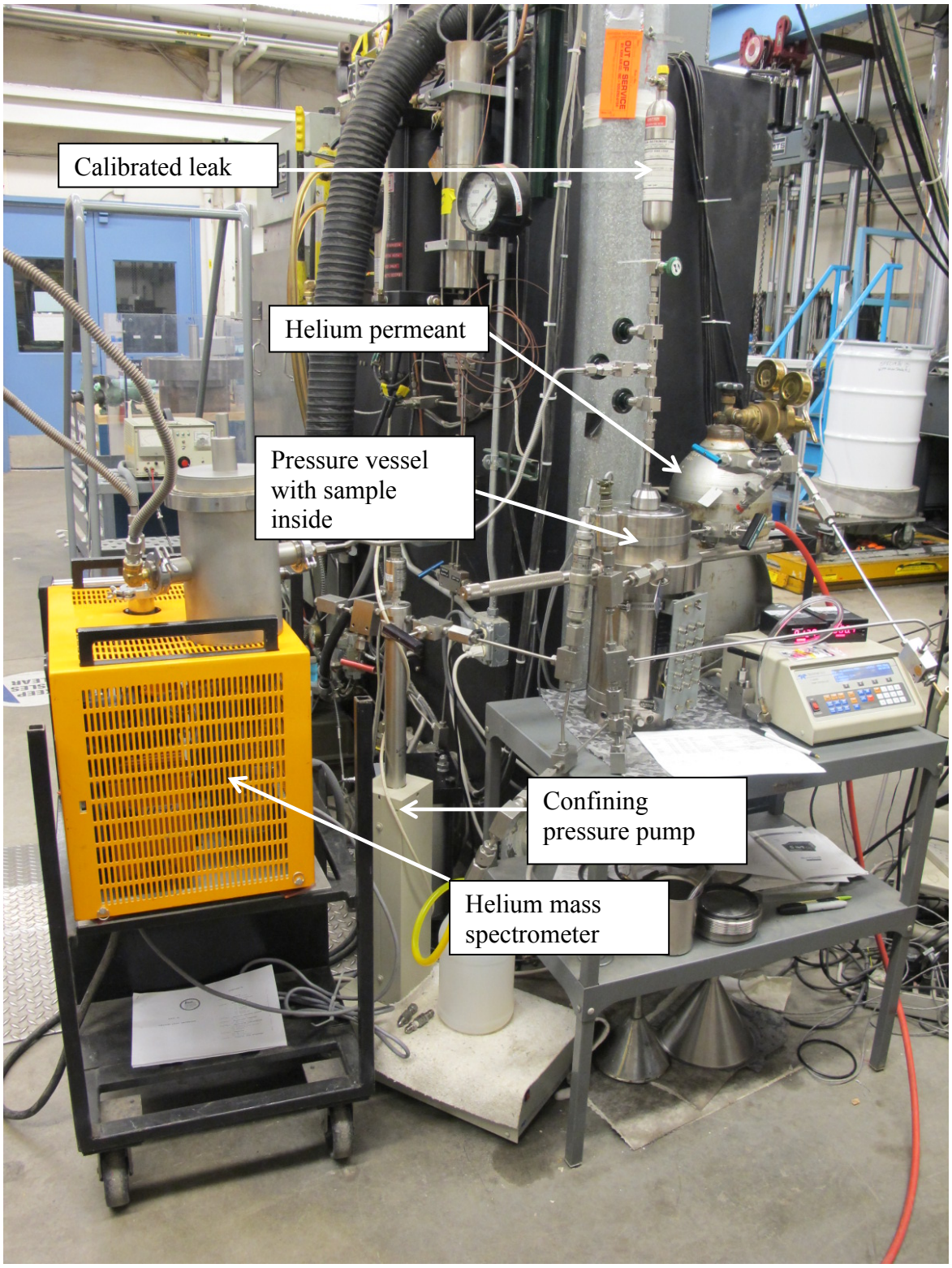

Figure 4. Permeability system.

2.2. Direct Shear properties

Direct shear tests to determine friction angle and cohesion on natural fractures were completed on 3 samples. Two of the samples were natural open fractures; the other fracture was separated using a gentle tap on a chisel using a ball peen hammer and chisel (Figure 5).

Figure 5. Healed fracture opened with a gentle tap.

The fracture surfaces were cut to approximately 3" X 2.5" X 1" height and cast in Hydrostone® and designated "top" and "bottom" where the top surface sits on top of the bottom surface in the direct shear machine (Figure 6 and Figure 7). The surfaces were then imaged using a 3D Digital Imaging Correlation (DIC) system. As shown in Figures 8, Figure 9, and Figure 10 the DIC imaging provided a topographical profile for both the top and bottom fracture surfaces and was used to create a tilt angle that was used to correct the normal and shear forces. The tilt angle indicates during shearing, if the sample is moving downhill or uphill. The "Y" axis is the direction of shear from left to right; as illustrated in Figure 11 a positive bottom slope indicates the top half of the fracture is going downhill. Figure 12, Figure 13, and Figure 14 show the tilt angle of the three surfaces for each direct shear test.

The three direct shear samples were each sheared at six different normal stresses. The normal stresses varied from 4 psi to 160 psi. The smallest normal stress was applied first then successively higher normal stresses applied thereafter with the exception of sample UE-19b 1021.0. For this sample, the first normal stress was 5 psi and the second was 3.9 psi followed by 18.7 psi, 40 psi, 80 psi, and 160 psi. This normal stress ordering was the result of an incorrect position of a valve on the machine. Because the initial stresses were low, running 5 psi followed by 3.9 psi is not deemed to be detrimental to the natural fracture surface of this sample even though this surface was the weakest of the three natural fracture shear samples.

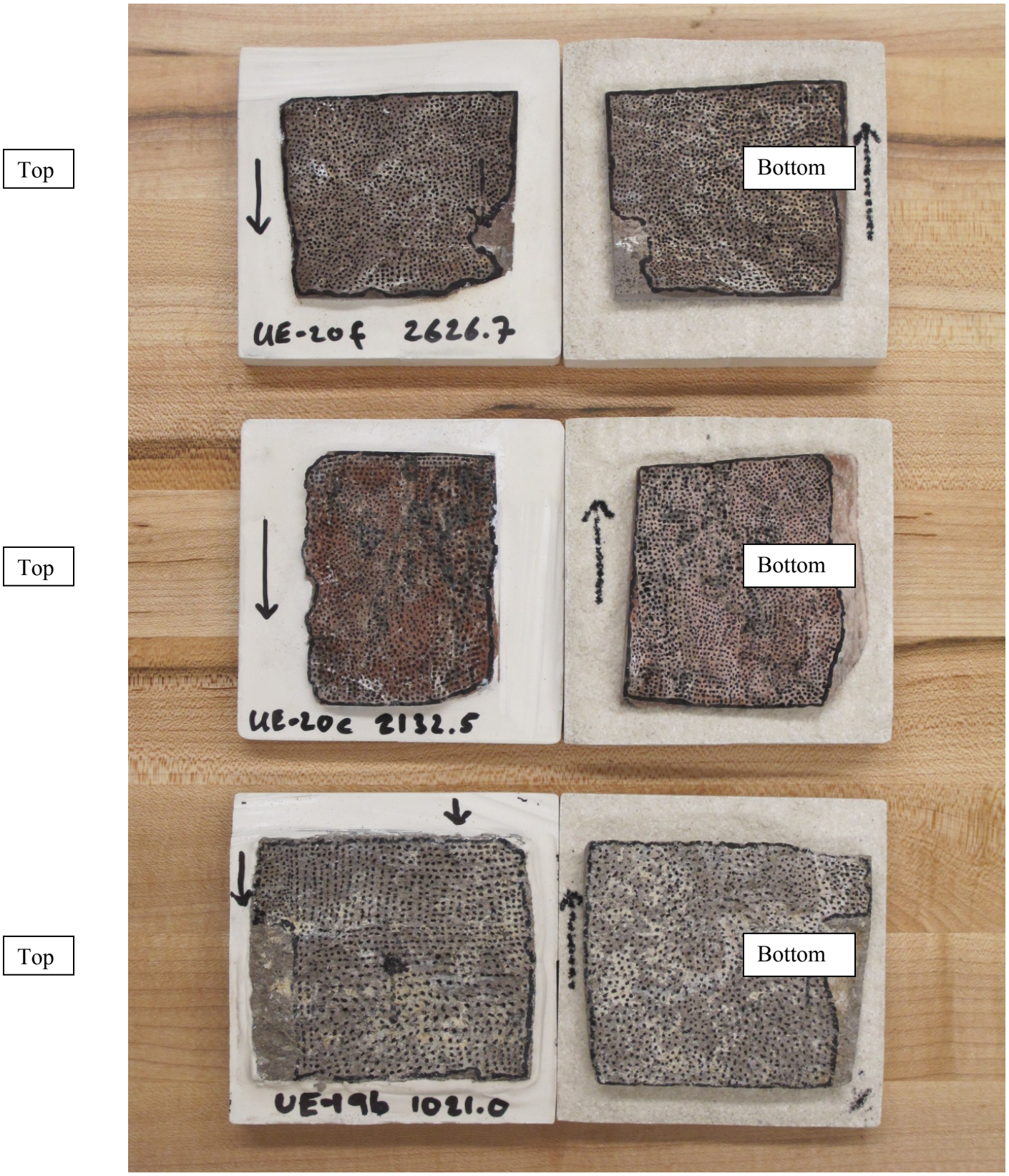

Figure 6. Direct shear sample cast for shearing in square shear box.

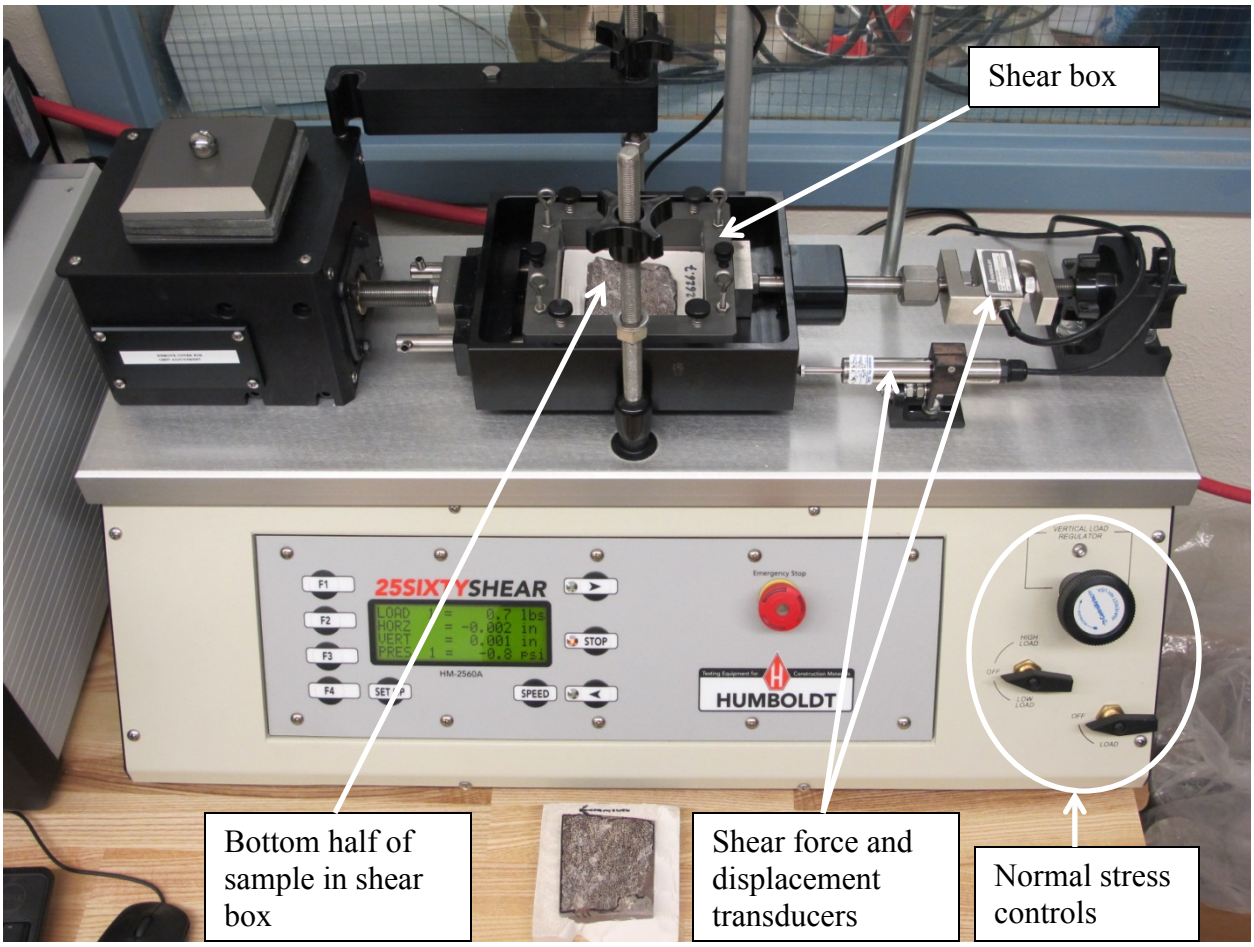

Figure 7. Direct shear test machine.

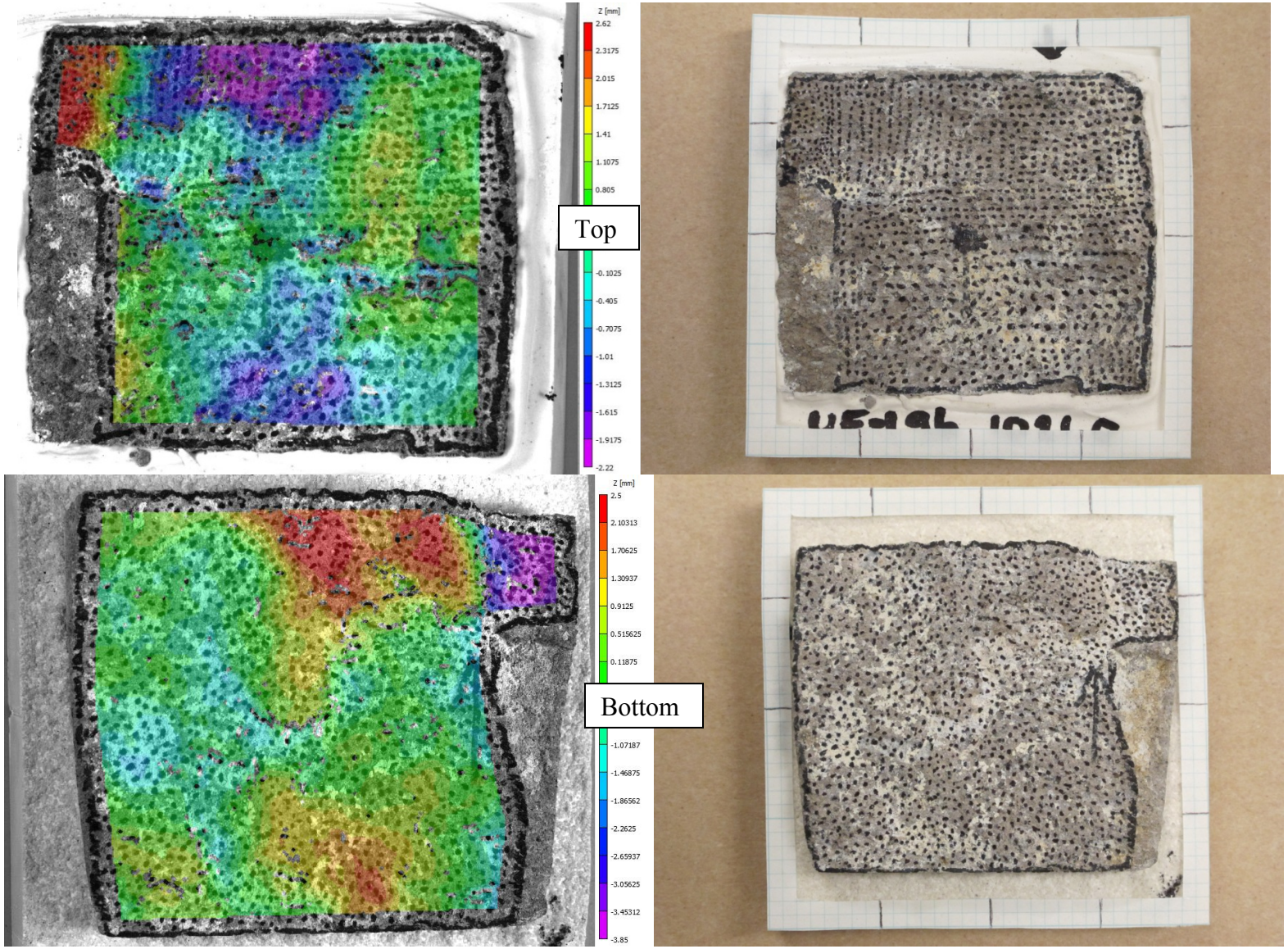

Figure 8. UE-19b_1021.0 elevation profile.

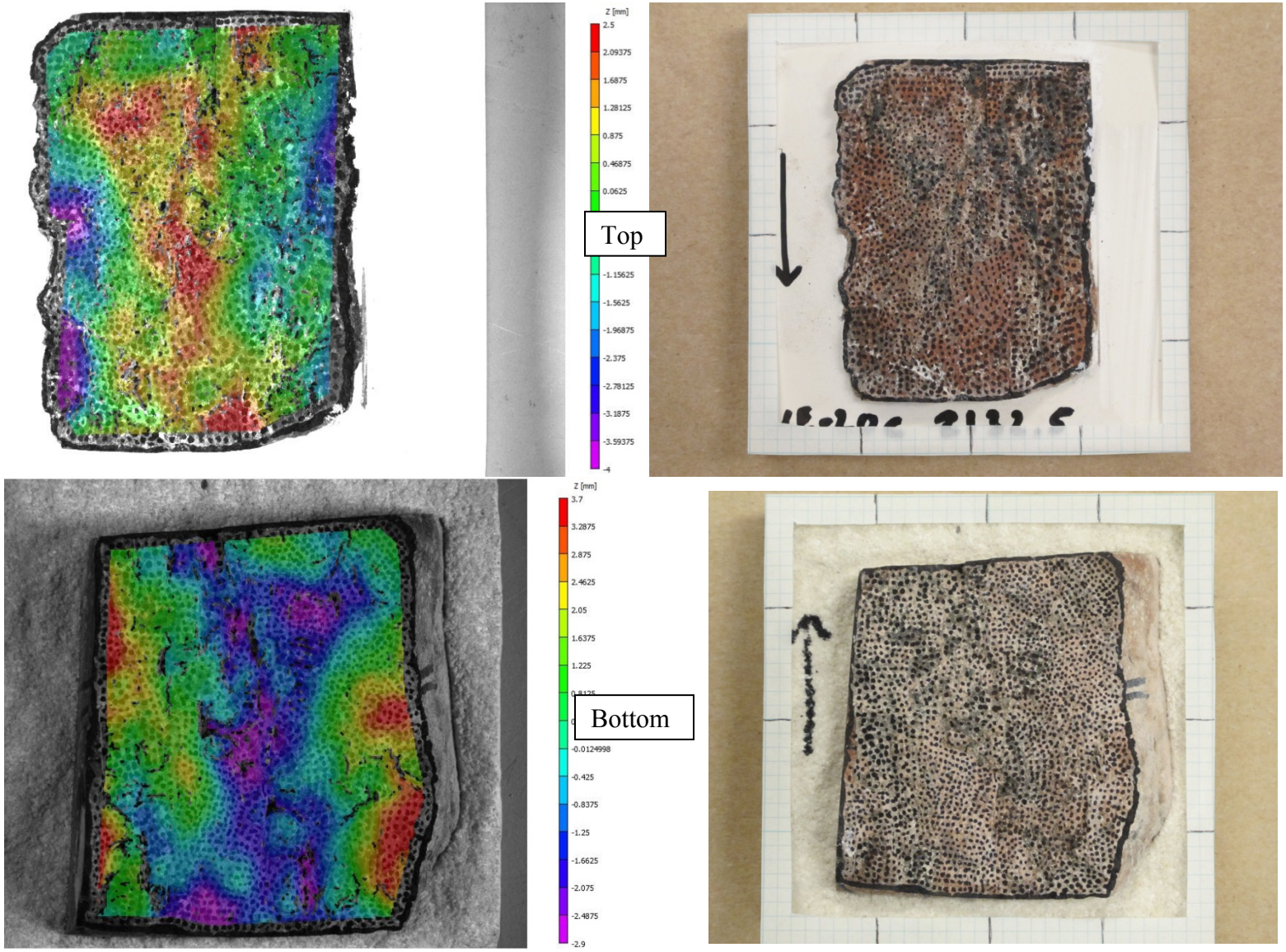

Figure 9. UE-20c_2132.5 elevation profile.

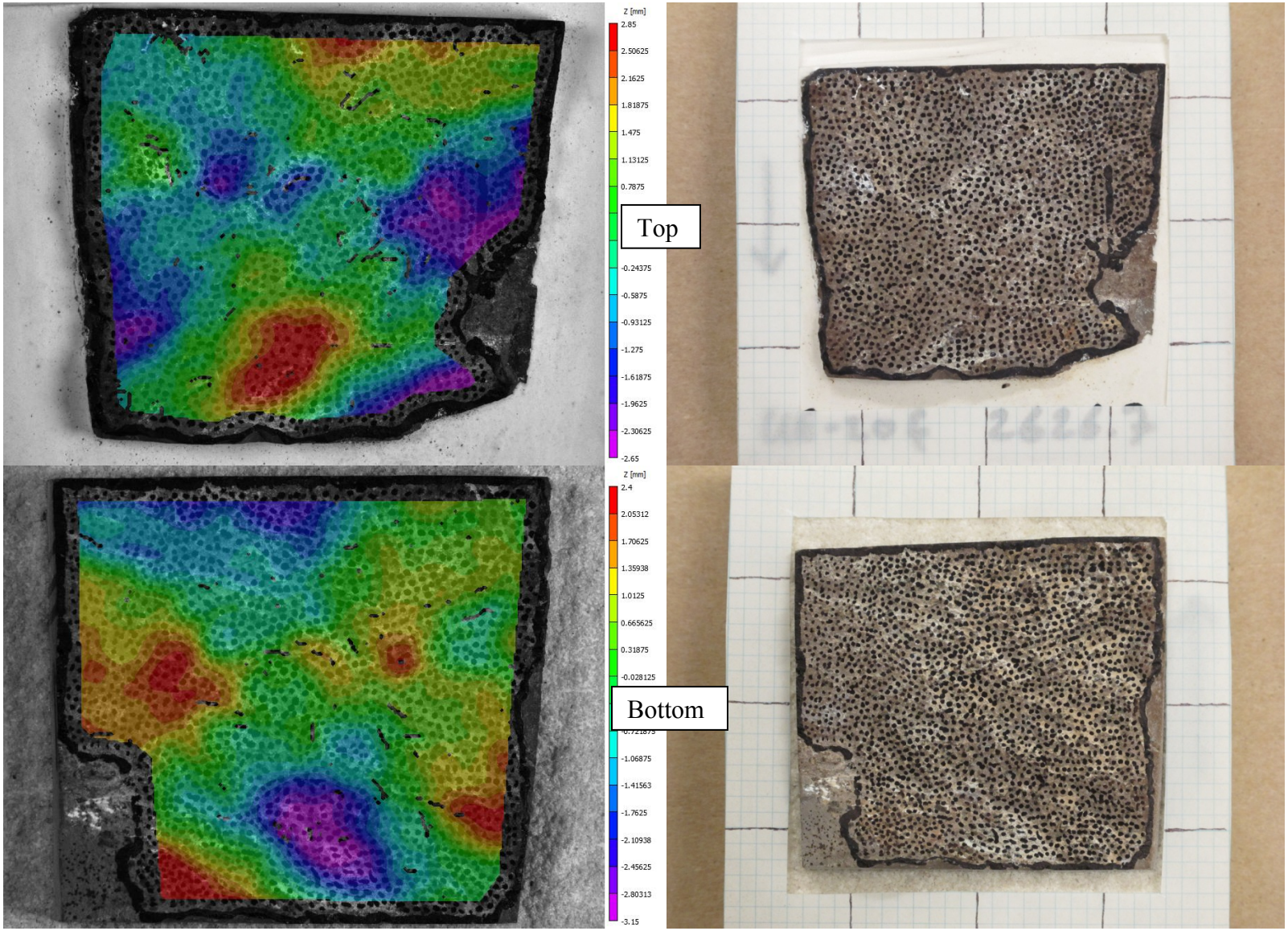

Figure 10. UE-20f_2626.7 elevation profile.

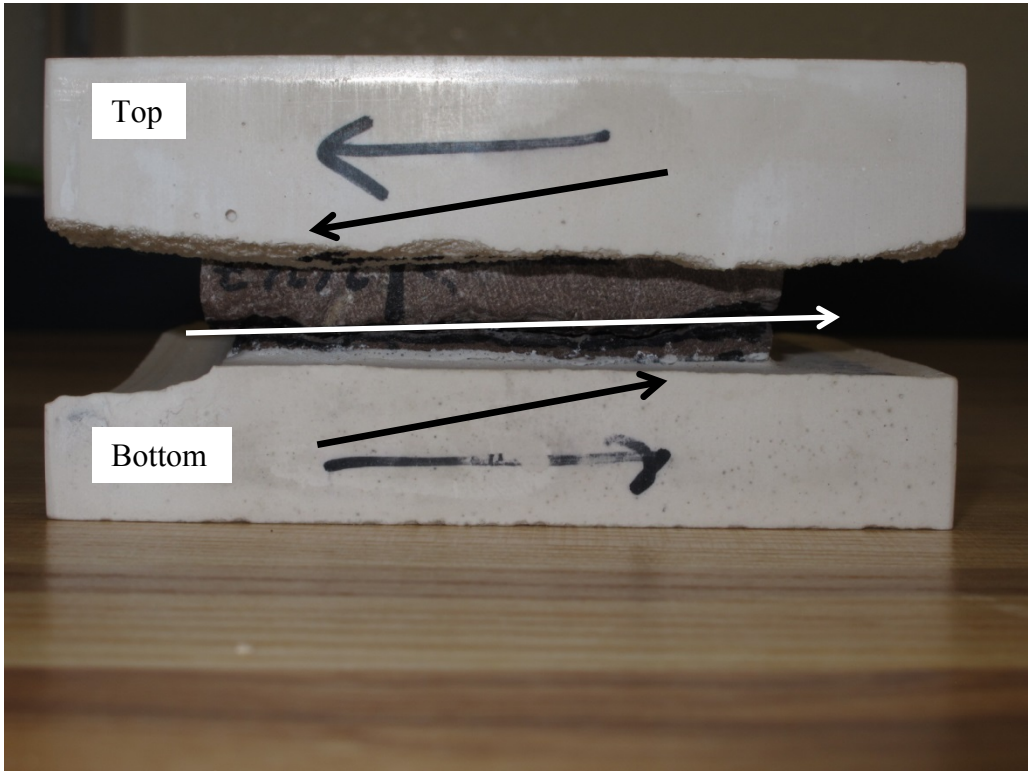

Figure 11. Example shear tilt angle for adjustment of normal and shear loads: top shearing downhill with positive bottom slope (black arrows show exaggerated slope angles to illustrate the shear tilt angle).

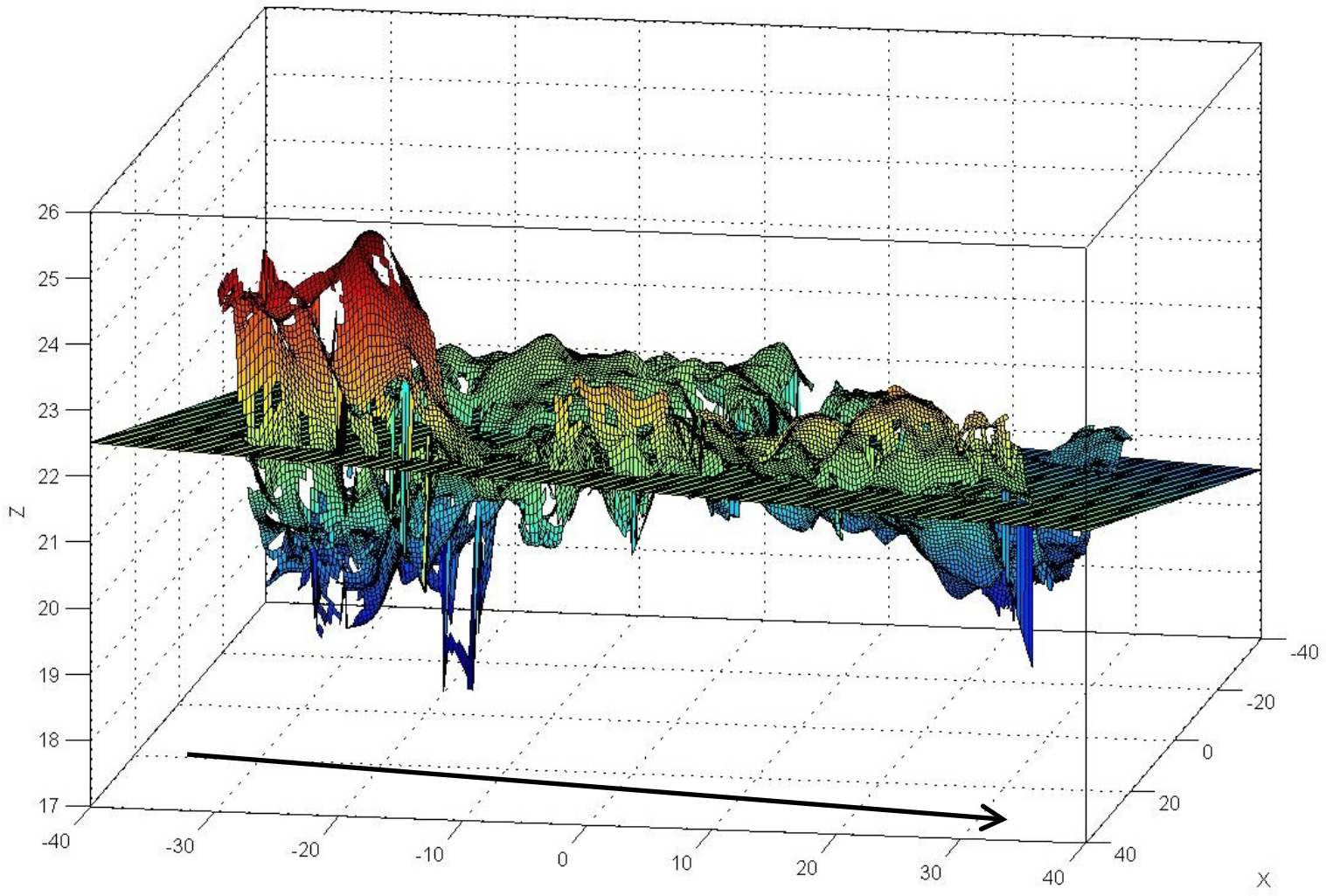

Figure 12. Shear angle -0.5715° for UE-19b 1021.0, bottom. Shear direction shown with arrow. Dimensions in mm. Vertical (Z) direction appears exaggerated for illustrative purposes. Surface varies less than 1 cm.

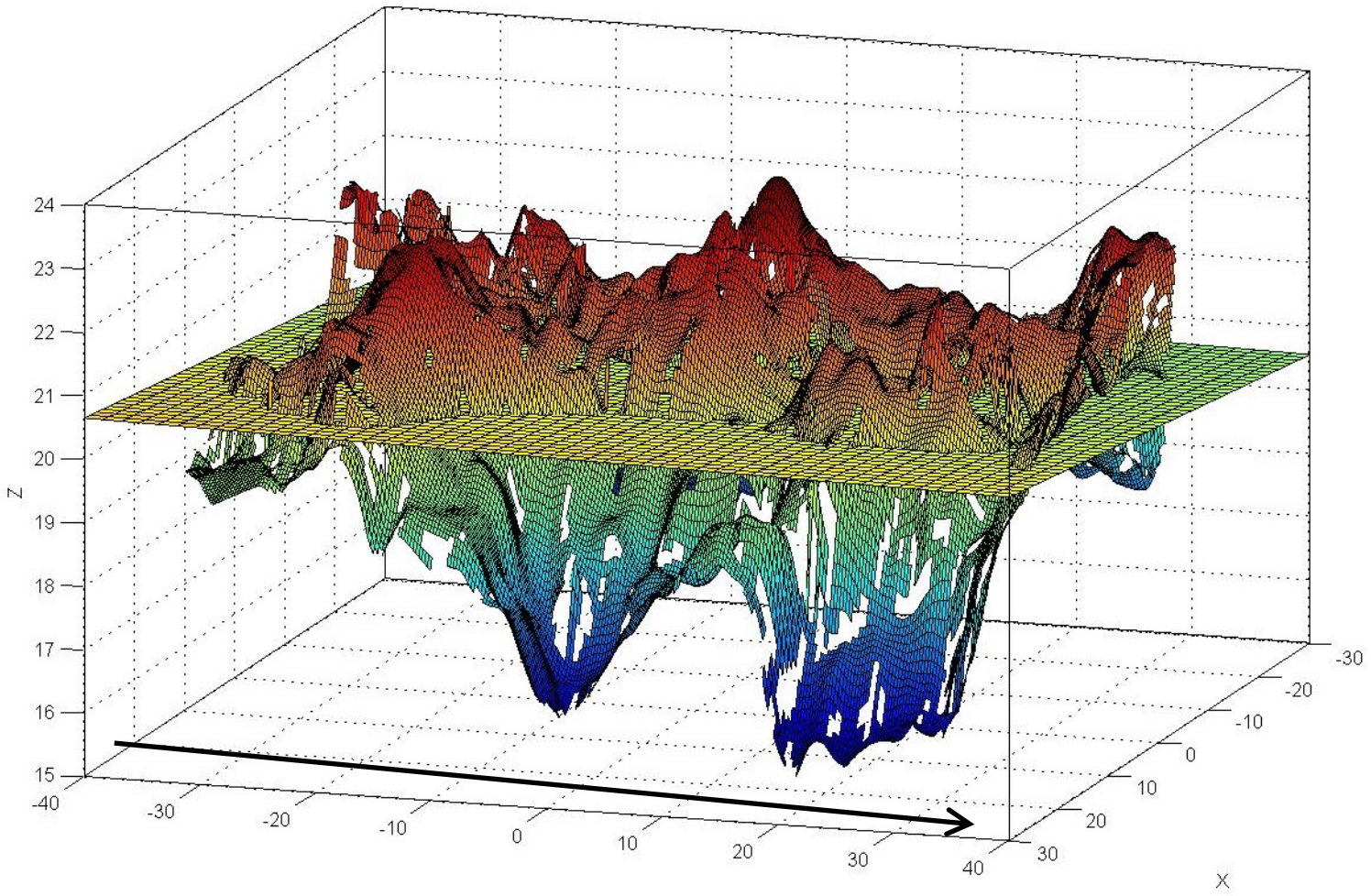

Figure 13. Shear angle -0.1659° for UE-20c 2132.5, bottom. Shear direction shown with arrow. Dimensions in mm. Vertical (Z) direction appears exaggerated for illustrative purposes. Surface varies less than 1 cm.

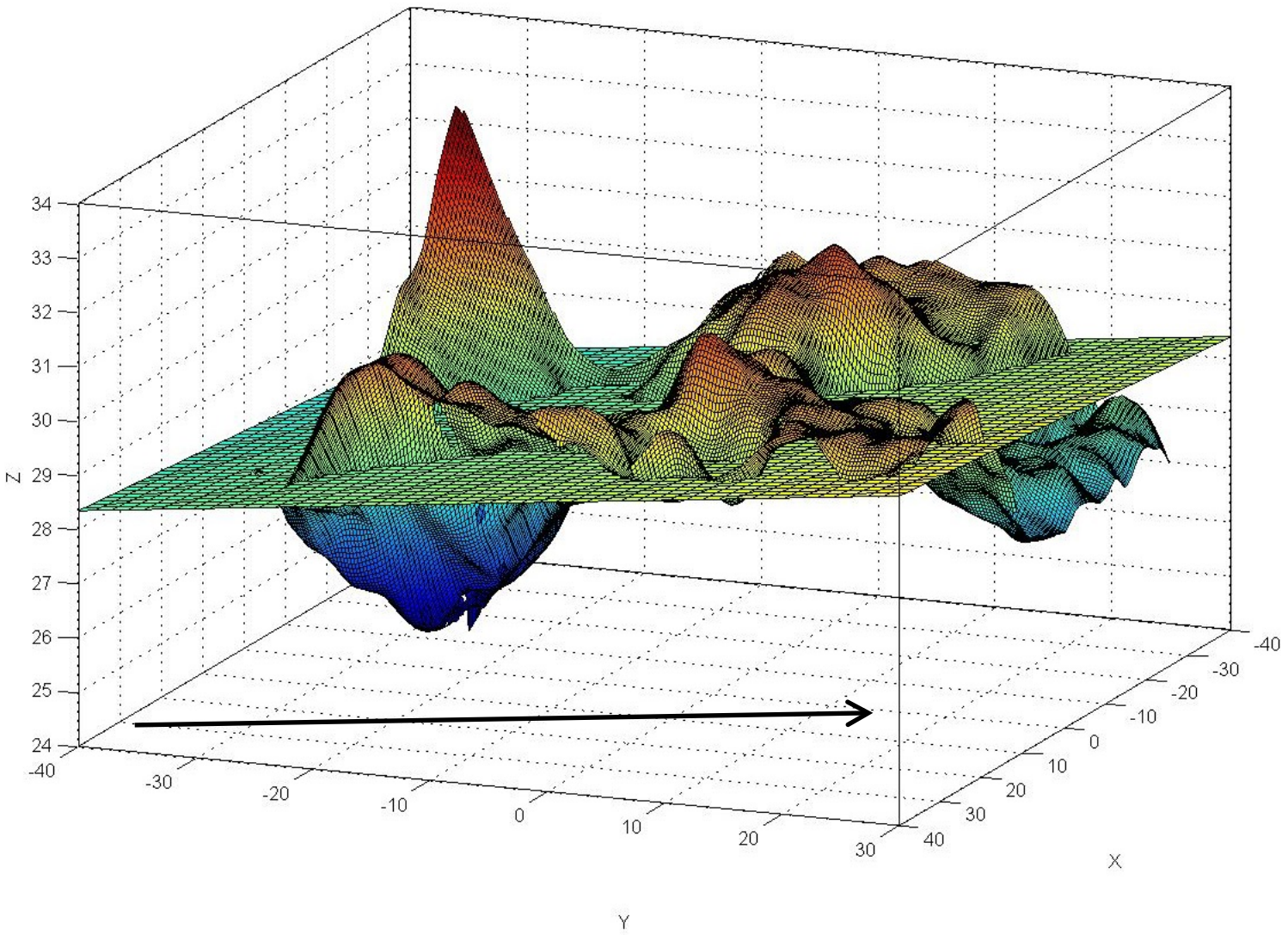

Figure 14. Shear angle 1.4161° for UE-20f 2626.7, top. Shear direction shown with arrow. Dimensions in mm. Vertical (Z) direction appears exaggerated for illustrative purposes. Surface varies less than 1 cm.

This page intentionally left blank.

3. EXPERIMENTAL RESULTS AND DISCUSSION

3.1. Permeability

Apparent permeability, k (in units of meters squared shown in the equation below and later converted to Darcys) was calculated from the following equation:

$$k = \frac{2\mu L Q_e P_{ea}}{A\left(P_{ia}^2 - P_{ea}^2\right)}$$

where:

μ is dynamic viscosity of the permeant (= 0.018×10^{-3} N· sec/m^2 and 0.020×10^{-3} N· sec/m^2 for nitrogen and helium respectively)
L = specimen length (in meters)
A = specimen cross-sectional area (in meters squared)
Q_e = steady-state permeant flow rate (in cubic meters per second)
P_{ia} and P_{ea} are the inlet and exit absolute pressures (in Pascals)

Table 1 contains sample number (composed of drill hole number and depth in feet), density (g/cc), confining pressure (MPa), and calculated permeability in Darcys. Measurements were made at five confining pressures for each sample; 500 psi, 1000 psi, 1500 psi, 2000 psi, and 2500 psi. The confining pressure effect is small and insignificant, likely because its value is small compared to the hydrostatic pore crush stress. Plots showing permeability and the flow conditions of all nine permeability samples are shown in Appendix A. Table 2 gives velocity measurements along with dynamic Young's modulus and Poisson's ratio for the permeability samples. The dynamic elastic Young's modulus, $E_{dynamic}$, was determined directly from:

$$E_{dynamic} = \frac{\rho V_S^2 \left(3V_P^2 - 4V_S^2\right)}{\left(V_P^2 - V_S^2\right)}$$

where ρ is the sample density and V_P and V_S are the longitudinal (P-wave) and shear (S-wave) velocities, respectively. Values of dynamic elastic Poisson's ratio, $\nu_{dynamic}$, were calculated from:

$$\nu_{dynamic} = \frac{\left(V_P^2 - 2V_S^2\right)}{2\left(V_P^2 - V_S^2\right)}$$

Table 1. Sample numbers, location, density, confining pressure and apparent permeability.

Sample	Hole	Depth (ft)	Density (g/cc)	Confining pressure (psi)	Apparent Permeability (Darcys)
UE-19b-349.0	UE-19b	349.0	1.20	500	6.2E-02
				1000	6.2E-02
				1500	5.9E-02
				2000	5.6E-02
				2500	4.3E-02
UE-19b-504.0	UE-19b	504.0	2.34	500	3.1E-04
				1000	2.1E-04
				1500	1.6E-04
				2000	1.2E-04
				2500	9.9E-05
UE-19b-1021.0	UE-19b	1021.0	2.33	500	7.5E-08
				1000	7.6E-08
				1500	7.0E-08
				2000	8.3E-08
				2500	8.1E-08
UE-19f-1987.9	UE-19f	1021.0	2.31	500	3.3E-07
				1000	2.9E-07
				1500	2.5E-07
				2000	2.3E-07
				2500	2.2E-07
UE-20c-654.4	UE-20c	654.4	2.29	500	4.7E-04
				1000	4.2E-04
				1500	3.8E-04
				2000	3.5E-04
				2500	3.1E-04
UE-20c-2127.0	UE-20c	2127.0	2.16	500	5.5E-05
				1000	5.4E-05
				1500	5.5E-05
				2000	5.3E-05
				2500	5.3E-05
UE-20c-2552.0	UE-20c	2552.0	1.53	500	1.5E-04
				1000	1.5E-04
				1500	1.4E-04
				2000	1.4E-04
				2500	1.4E-04

Table 1, con't. Sample numbers, location, density, confining pressure and apparent permeability.

UE-20f-2627.7	UE-20f	2627.7	2.26	500	8.2E-08
				1000	8.4E-08
				1500	8.6E-08
				2000	8.0E-08
				2500	9.3E-08
UE-19b-832.8	UE-19b	832.8	2.21	500	6.1E-04
				1000	5.5E-04
				1500	5.3E-04
				2000	4.9E-04
				2500	4.7E-04

This page intentionally left blank.

Table 2. P and S wave Velocity, Dynamic Young's modulus and Poisson's ratio for permeability samples.

			Axial				Lateral			
Sample	**Rock type**	Density (g/cc)	P velocity (m/s)	S velocity (m/s)	*E* dynamic (Gpa)	ν Dynamic	P velocity (m/s)	S velocity (m/s)	*E* dynamic (Gpa)	ν Dynamic
ue-19b 349.0-349.4 (subcore from permeability sample)	Nonwelded TMR	1.20	1256	732	1.60	0.24	N/A	N/A	N/A	N/A
ue-19b 504.0-504.8	Moderately welded TMR	2.34	2189	1193	8.57	0.29	2074	1244	8.81	0.22
ue-19b 1021.0-1021.8	Moderately welded TMR	2.33	5043	3208	55.53	0.16	5201	3060	53.80	0.24
ue-19f 1987.0-1987.9	Strongly welded Scrugham Peak rhyolite	2.31	4515	2839	43.77	0.17	4112	2561	35.93	0.18
ue-20c 654.4-654.9	Welded TMR	2.29	2910	1634	15.50	0.27	3319	1920	21.03	0.25
ue-20c 2127.0-2127.4	Strongly welded Tiva Canyon Tuff	2.16	3636	2226	25.75	0.20	3950	2219	27.06	0.27
ue-20c 2552.0-2552.5	Nonwelded Tiva Canyon Tuff	1.53	2691	1687	10.23	0.18	3190	1670	11.18	0.31
ue-20f 2627.4-2627.7	Strongly welded Tiva Canyon Tuff	2.26	4555	2843	43.16	0.18	4628	2835	43.60	0.20
ue-19b 832.8-833.5	Moderaltely welded TMR with lithophysae	2.21	2942	1593	14.52	0.29	2992	1888	18.43	0.17

This page intentionally left blank.

Figure 15 and Figure 16 show the relationship of permeability to confining pressure and density respectively of the nine samples tested. For both plots, in general, permeability decreases with increasing confining pressure and density. The effect of confining pressure on permeability is small (at the most half an order of magnitude over the range of confining pressures tested) whereas the effect of density on permeability is up to six orders of magnitude within the nine samples tested.

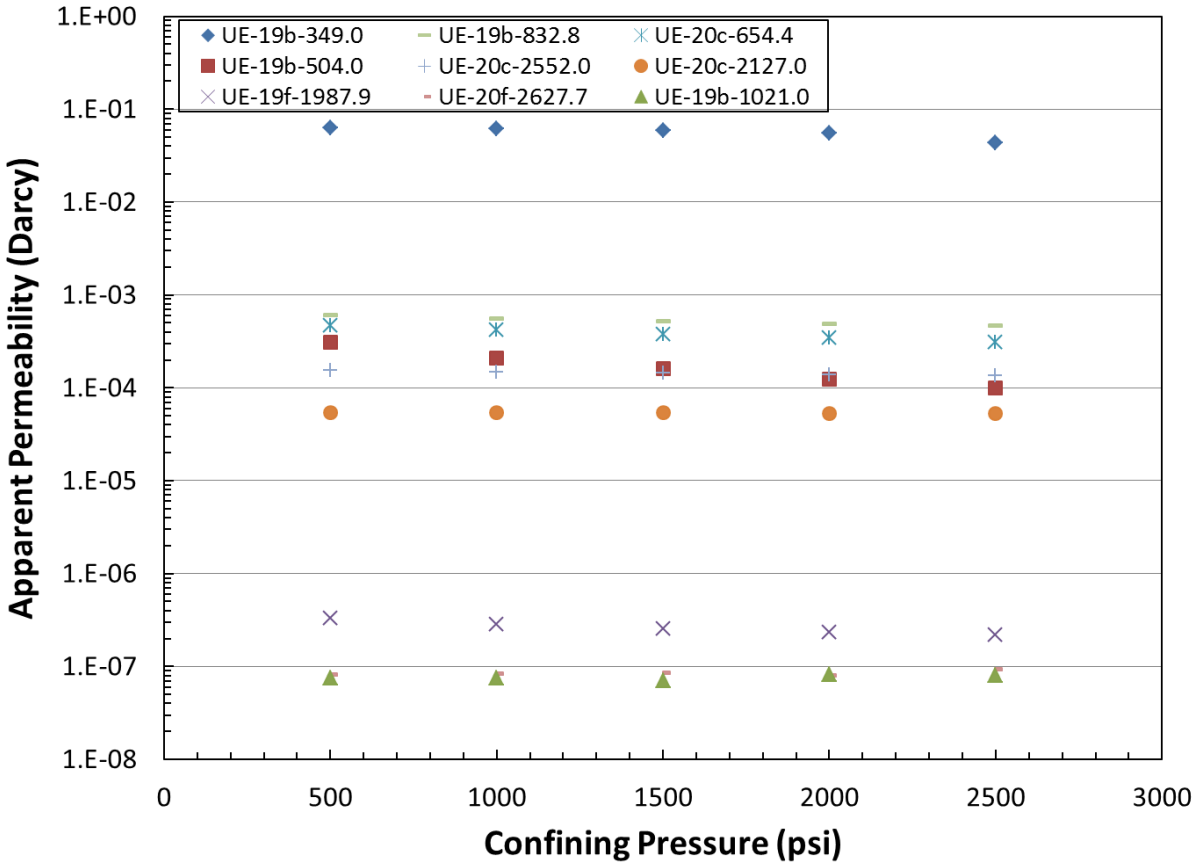

Figure 15. Permeability versus confining pressure.

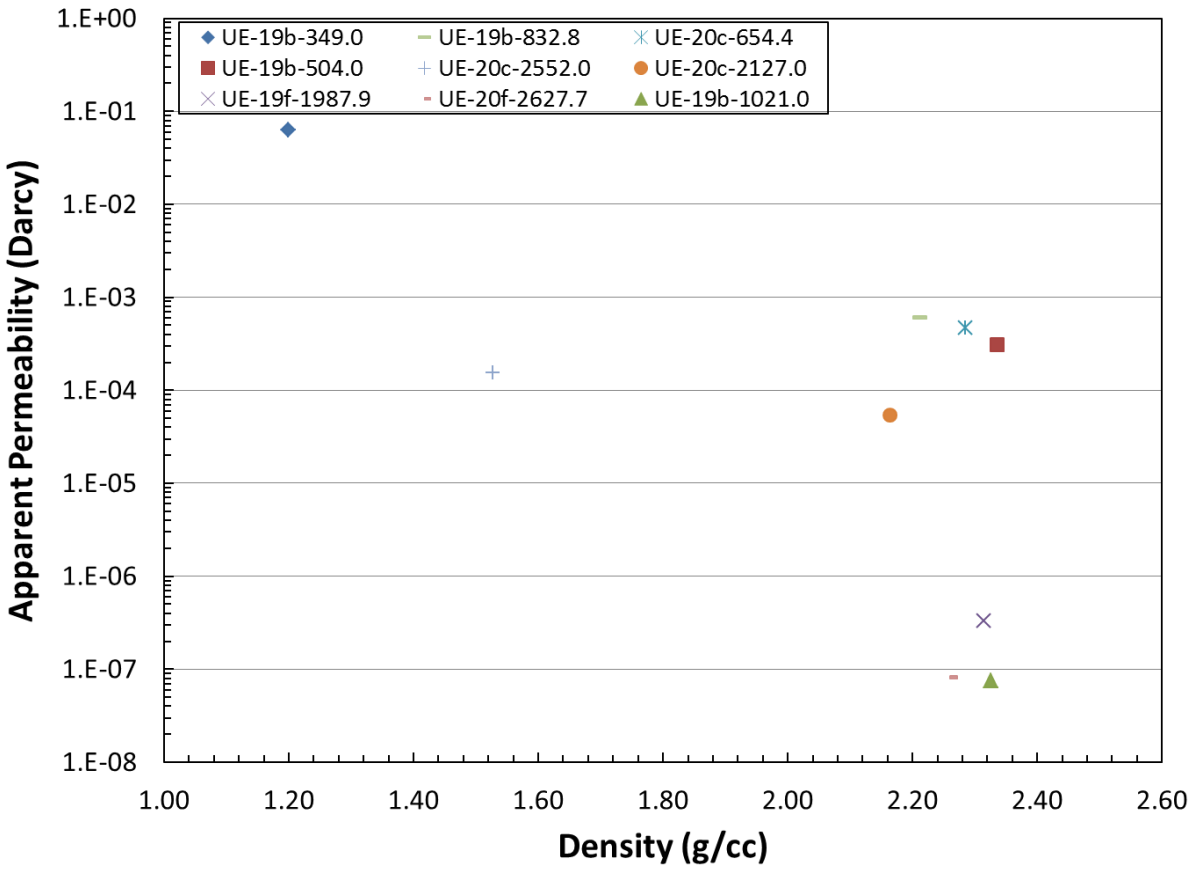

Figure 16. Permeability versus density.

Figure 17, Figure 18, Figure 19, and Figure 20 show the relationship of density to P and S wave velocity, dynamic Young's modulus and Poisson's ratio. P and S wave velocities were chosen only from the axial measurement direction. P and S wave velocity and dynamic Young's modulus generally increase with increasing density and a best fit line is given for these relationships. Dynamic Poisson's ratio ranges from 0.15 to 0.30 for all samples.

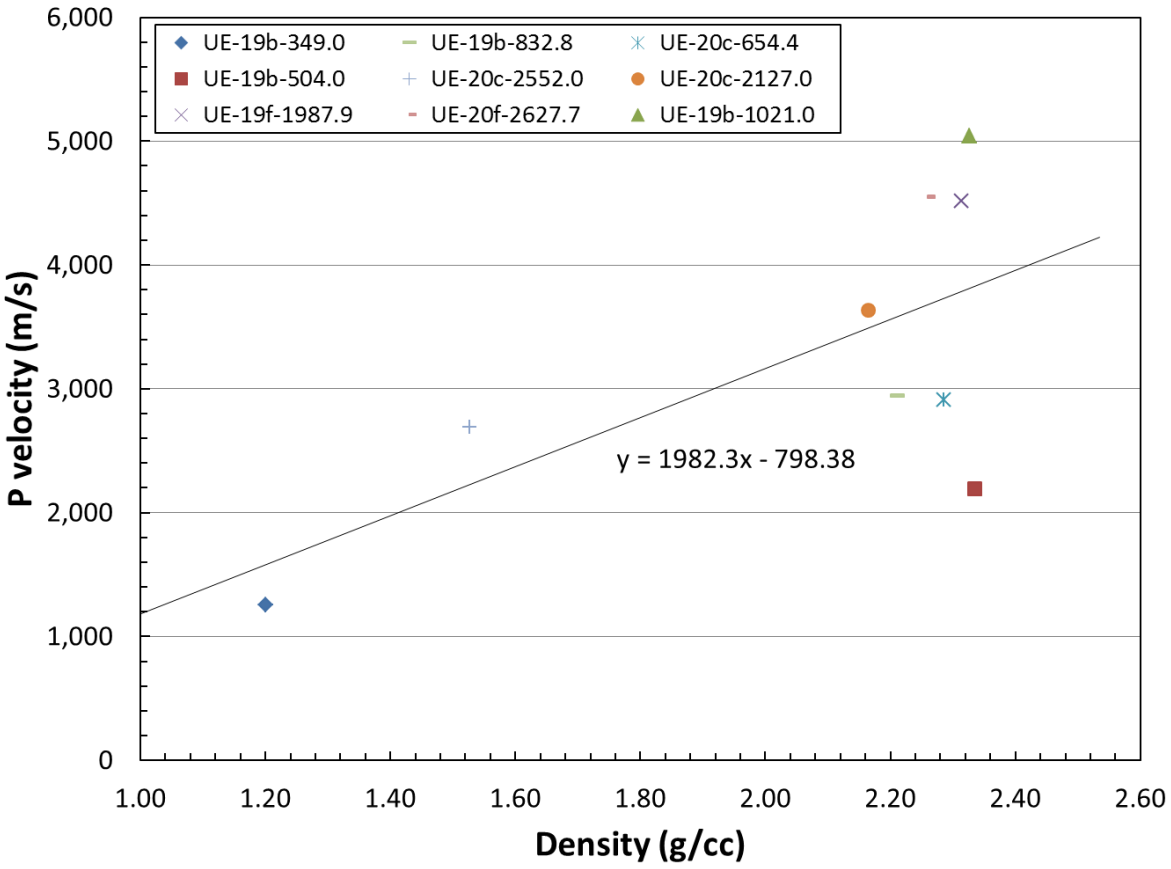

Figure 17. P velocity versus density.

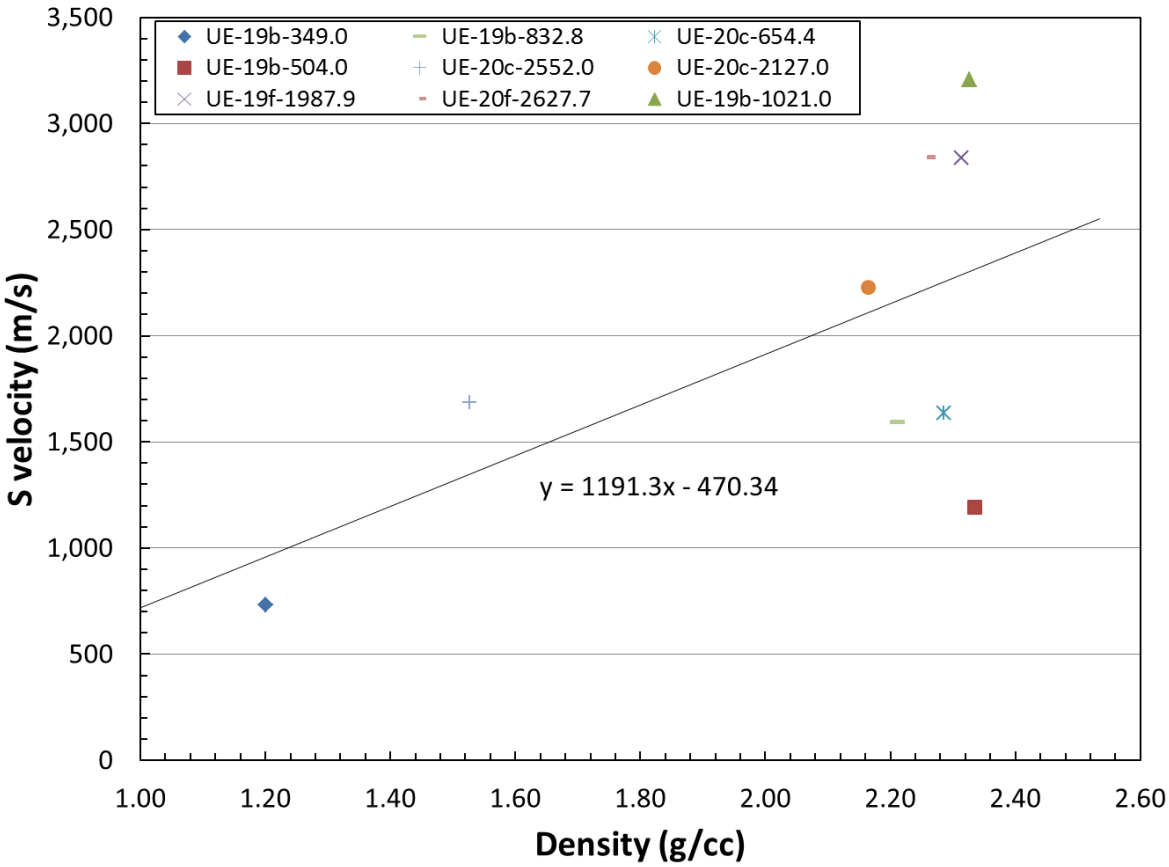

Figure 18. S velocity versus density.

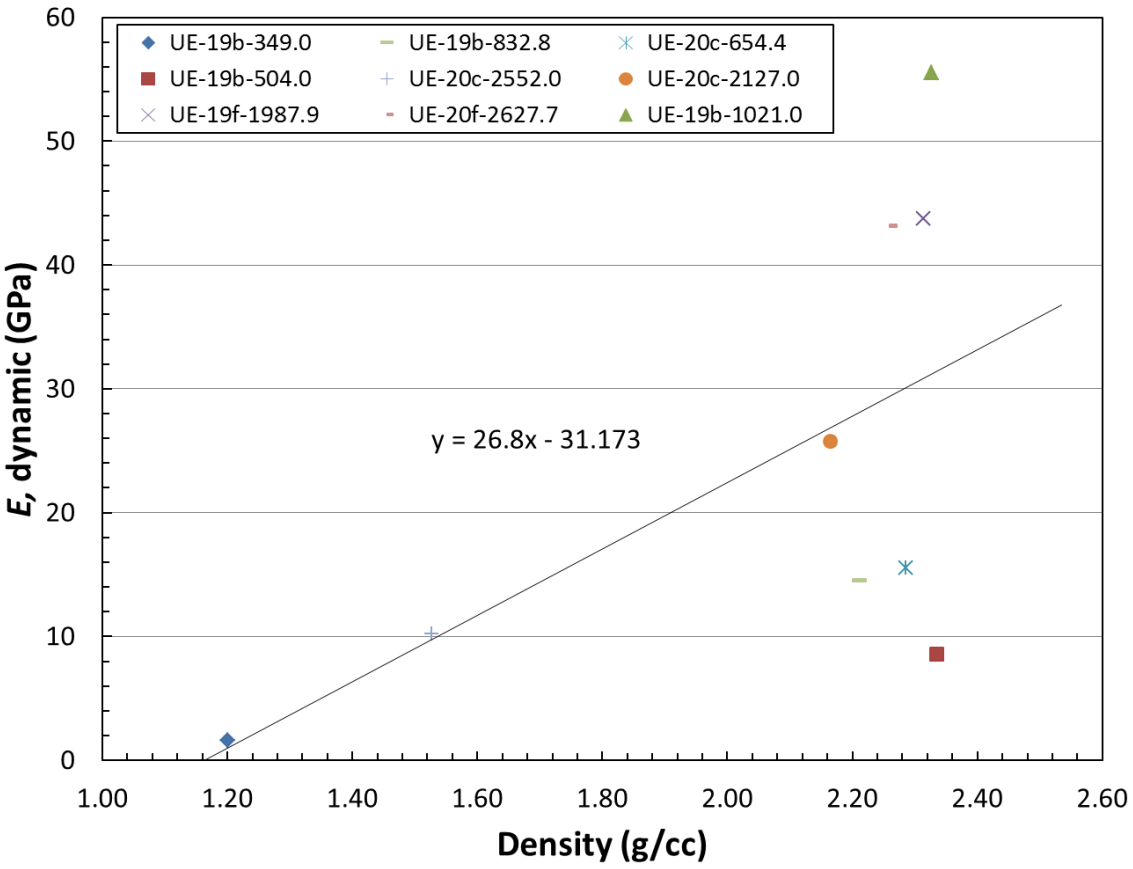

Figure 19. Dynamic Young's modulus versus density.

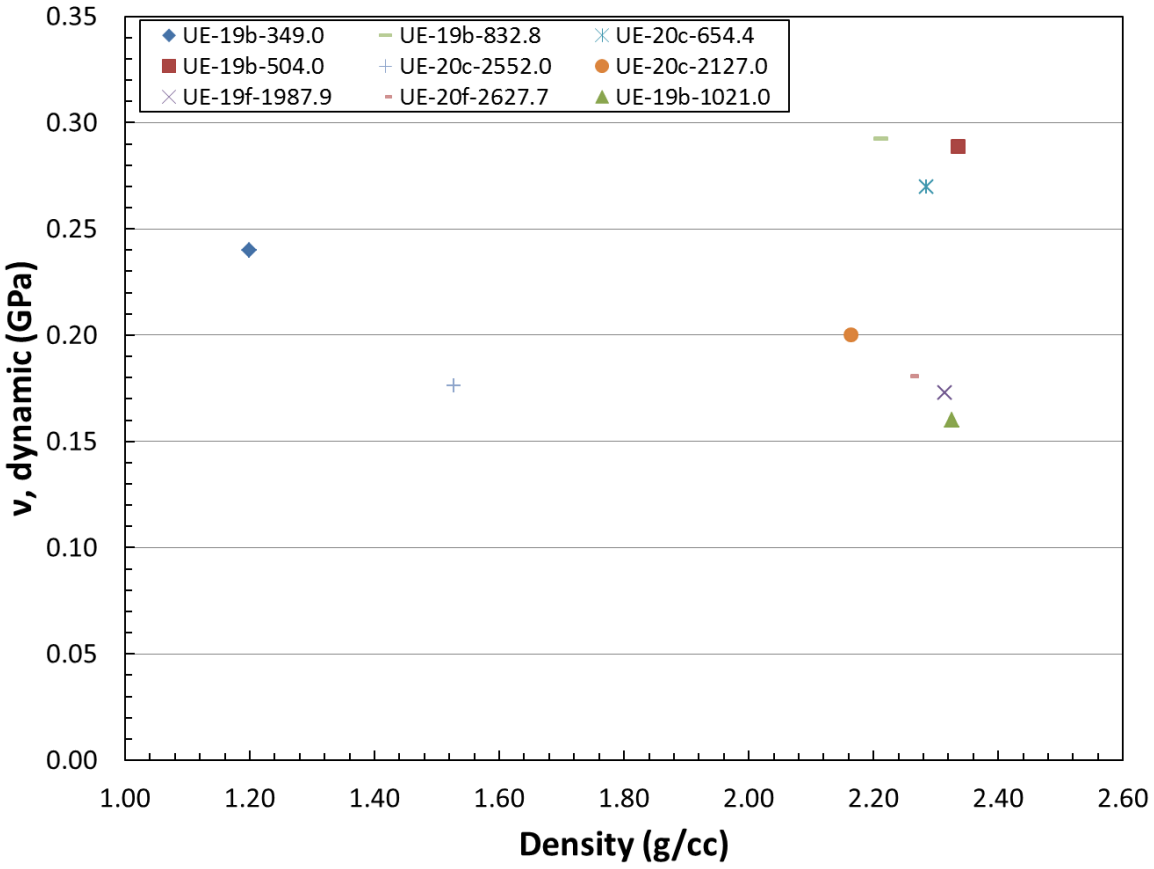

Figure 20. Dynamic Poisson's ratio versus density.

3.2. Direct Shear

Plots of shear force versus horizontal displacement for the three direct shear samples are shown in Figure 21, Figure 22, and Figure 23. Each of these figures shows all six traces. Residual shear force is labeled with a blue circle and peak shear force (when a peak is significantly distinct from the residual force) is labeled with a red square. Residual shear force is picked based on two criteria; 1) when shear force is constant for ~0.02 inches of horizontal displacement and 2) either after the shear force reaches peak level or after the shear force becomes nearly constant with increasing horizontal displacement. The latter criterion is typically chosen after >0.05 inches of horizontal displacement. Table 3 lists normal load, displacement, shear load, shear area, normal stress, and shear stress. Shear area is calculated assuming a rectangular specimen shape factoring in the displacement at either the residual or peak point selection. Normal and shear stress are adjusted for the shear angle (Tilt) by using the following relationships:

Adjusted normS = normS * Cos(Tilt) - shearS * Sin(Tilt)
Adjusted shearS = shearS * Cos(Tilt) + normS * Sin(Tilt)

Where Adjusted normS and Adjusted shearS are normal and shear stresses corrected for either upward or downward shearing and normS and shearS are normal and shear stresses taking normal and shear load divided by the sample area at the residual or peak point of interest.

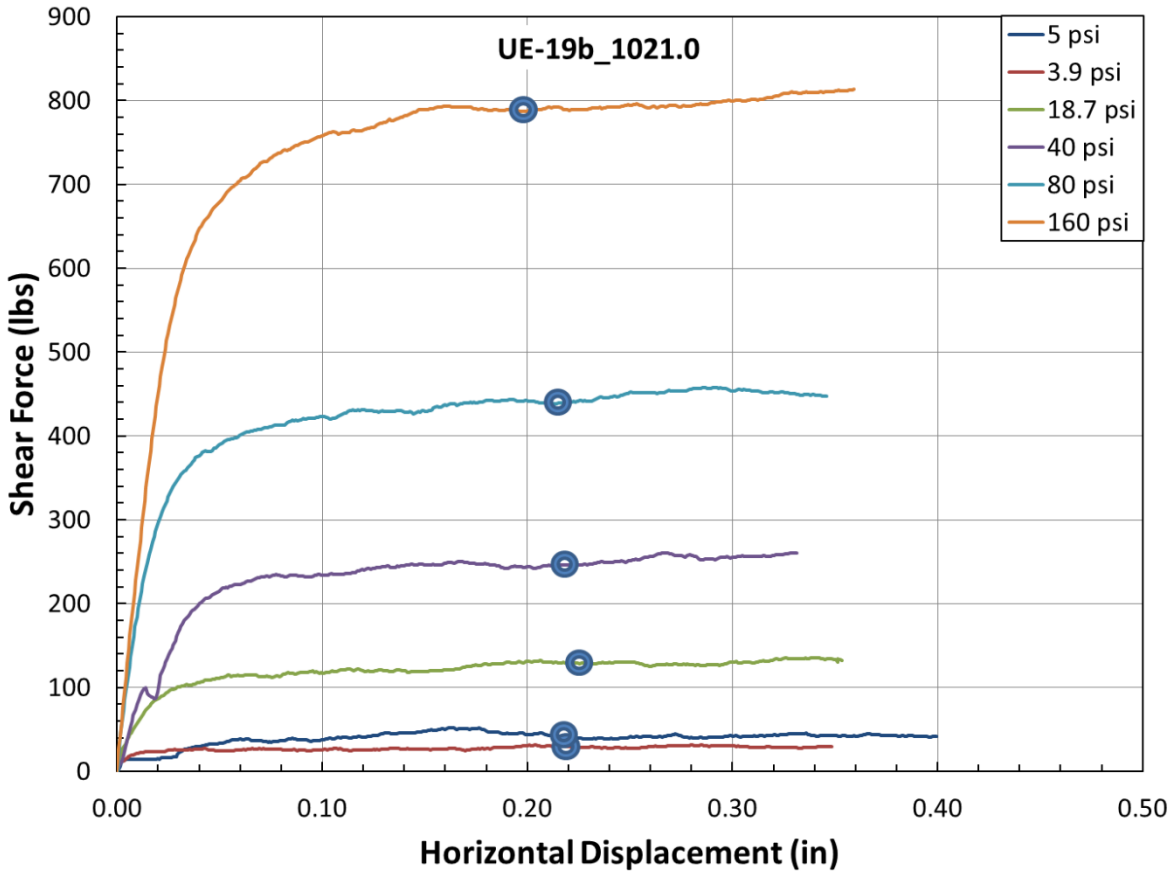

Figure 21. Shear force versus displacement for UE-19b 1021.0

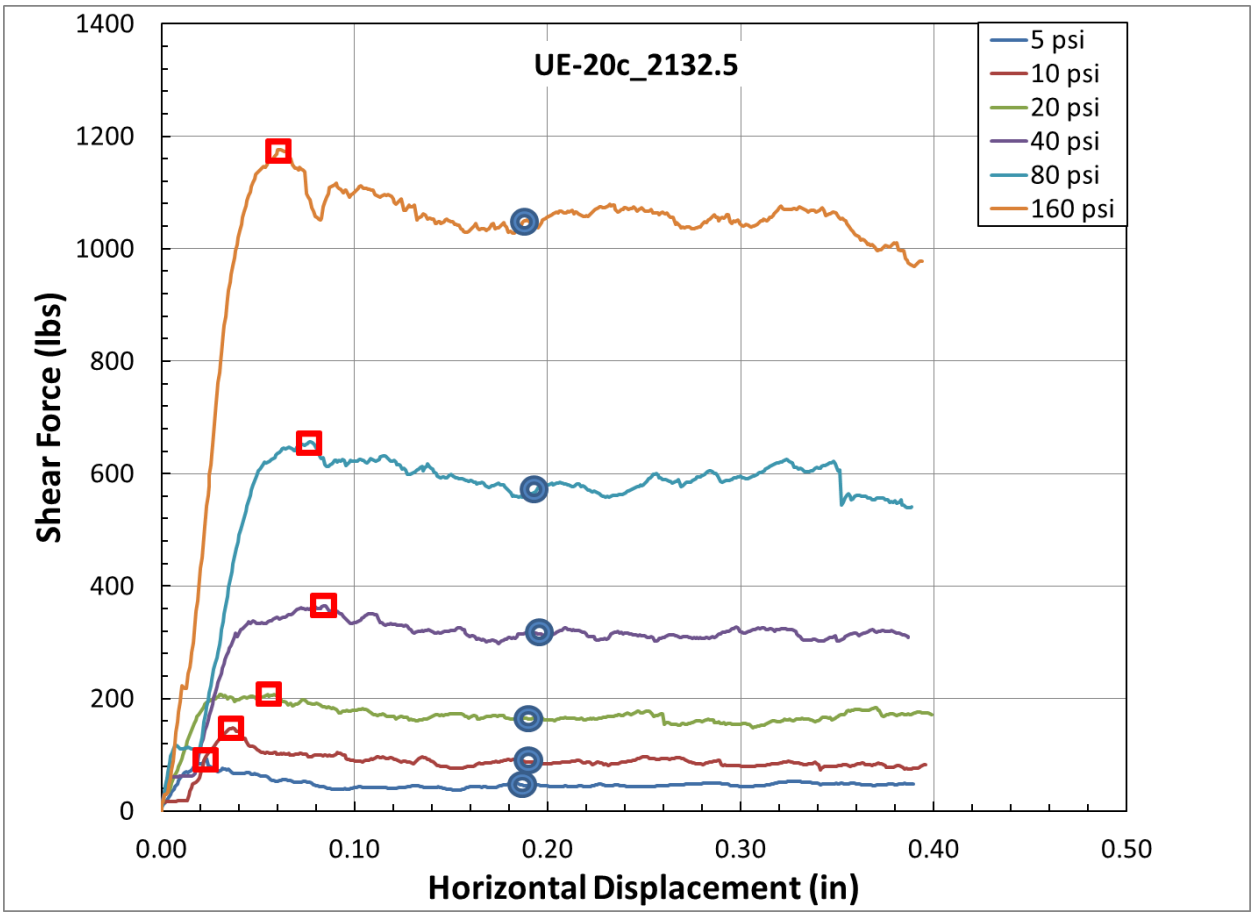

Figure 22. Shear force versus displacement for UE-20c 2132.5

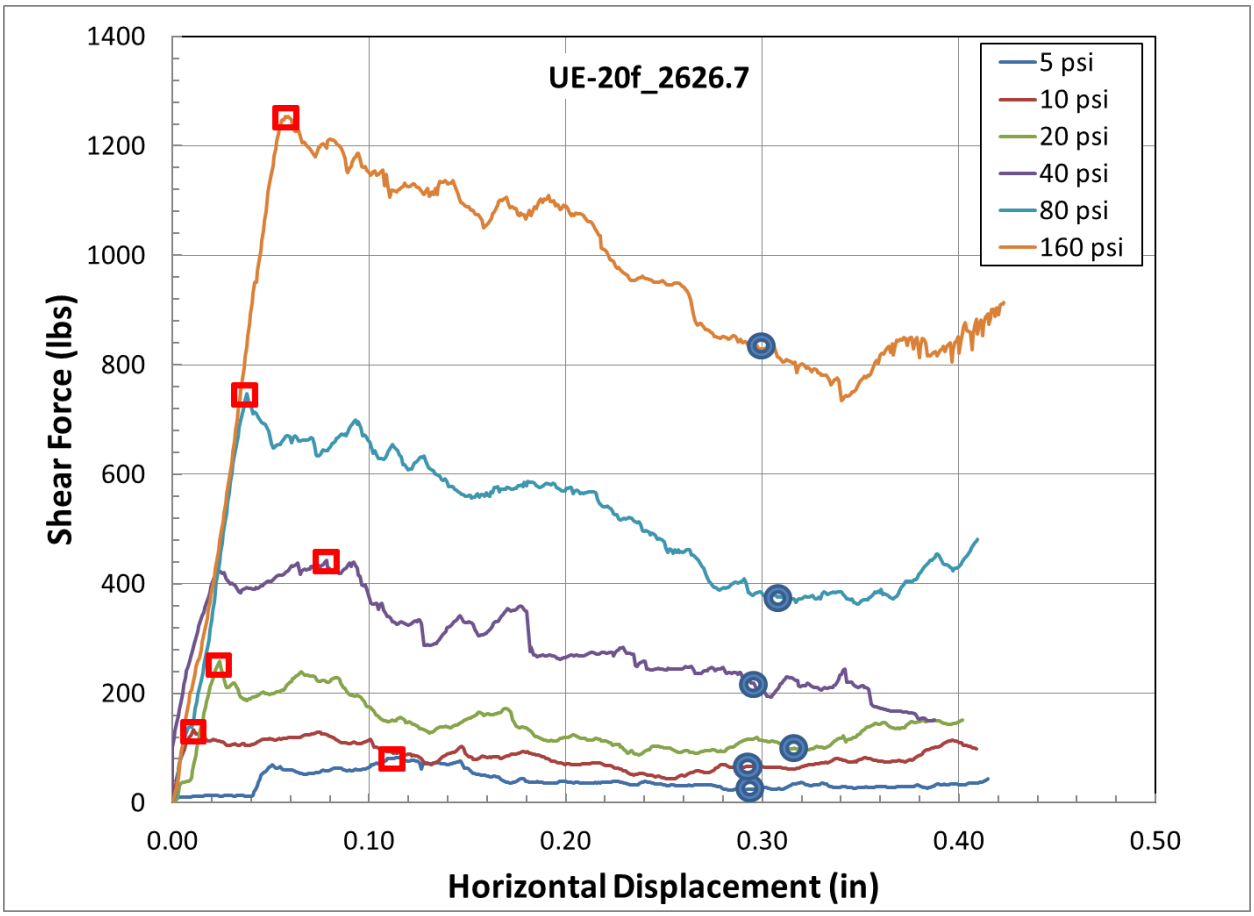

Figure 23. Shear force versus displacement for UE-20f 2626.7

Table 3. Normal load, Displacement, Shear load, Shear area, Normal stress and Shear stress for direct shear residual points.

UE-19b_1021.0 Residual					
Normal load (lbs)	Displacement (in)	Shear load (lbs)	Shear area (in2)	Normal Stress (psi)	Shear Stress (psi)
44.4	0.219	29.3	7.69	5.8	3.8
35.0	0.218	30.1	7.70	4.6	3.9
166.0	0.224	128.9	7.68	21.8	16.6
355.4	0.218	246.4	7.70	46.5	31.6
710.7	0.214	438.8	7.71	92.8	56.0
1421.4	0.199	787.3	7.75	184.4	99.7
UE-20c 2132.5 Residual					
Normal load (lbs)	Displacement (in)	Shear load (lbs)	Shear area (in2)	Normal Stress (psi)	Shear Stress (psi)
32.4	0.184	49.1	6.01	5.4	8.2
64.8	0.190	86.6	5.99	10.9	14.4
129.5	0.190	163.9	5.99	21.7	27.3
259.0	0.196	314.4	5.98	43.5	52.5
518.0	0.193	566.2	5.98	86.8	94.4
1036.0	0.185	1038.6	6.00	173.0	172.5
UE-20f 2626.7 Residual					
Normal load (lbs)	Displacement (in)	Shear load (lbs)	Shear area (in2)	Normal Stress (psi)	Shear Stress (psi)
31.2	0.294	24.1	5.50	5.8	4.2
62.4	0.292	66.5	5.51	11.6	11.8
124.7	0.317	98.8	5.44	23.4	17.6
249.4	0.296	211.8	5.50	46.3	37.4
498.9	0.309	376.0	5.46	93.0	66.5
997.8	0.300	828.4	5.49	185.5	146.4

Table 3, con't. Normal load, Displacement, Shear load, Shear area, Normal stress and shear stress for direct shear peak points

UE-20c 2132.5 Peak					
Normal load (lbs)	Displacement (in)	Shear load (lbs)	Shear area (in2)	Normal Stress (psi)	Shear Stress (psi)
32.4	0.024	93.8	6.41	5.1	14.6
64.8	0.037	147.7	6.38	10.2	23.1
129.5	0.058	207.4	6.33	20.6	32.7
259.0	0.084	365.3	6.26	41.5	58.2
518.0	0.077	656.3	6.28	82.8	104.3
1036.0	0.062	1175.9	6.32	164.5	185.7
UE-20f 2626.7 Peak					
Normal load (lbs)	Displacement (in)	Shear load (lbs)	Shear area (in2)	Normal Stress (psi)	Shear Stress (psi)
31.2	0.116	82.2	5.95	5.6	13.7
62.4	0.011	133.3	6.21	10.6	21.2
124.7	0.024	258.0	6.18	21.2	41.3
249.4	0.078	442.8	6.04	43.1	72.3
498.9	0.038	748.1	6.14	84.2	119.8
997.8	0.059	1253.4	6.09	168.9	201.8

Once the corrected (for sample area and tilt) normal and shear stresses are determined for each trace of the three direct shear tests (Table 3), these points can be plotted in Shear stress versus Normal stress space as shown in Figure 24, Figure 25, and Figure 26. The arctangent of the slope of the best fit line in this stress space gives the friction angle of the fracture surface and the "Y" intercept gives the cohesion in psi.

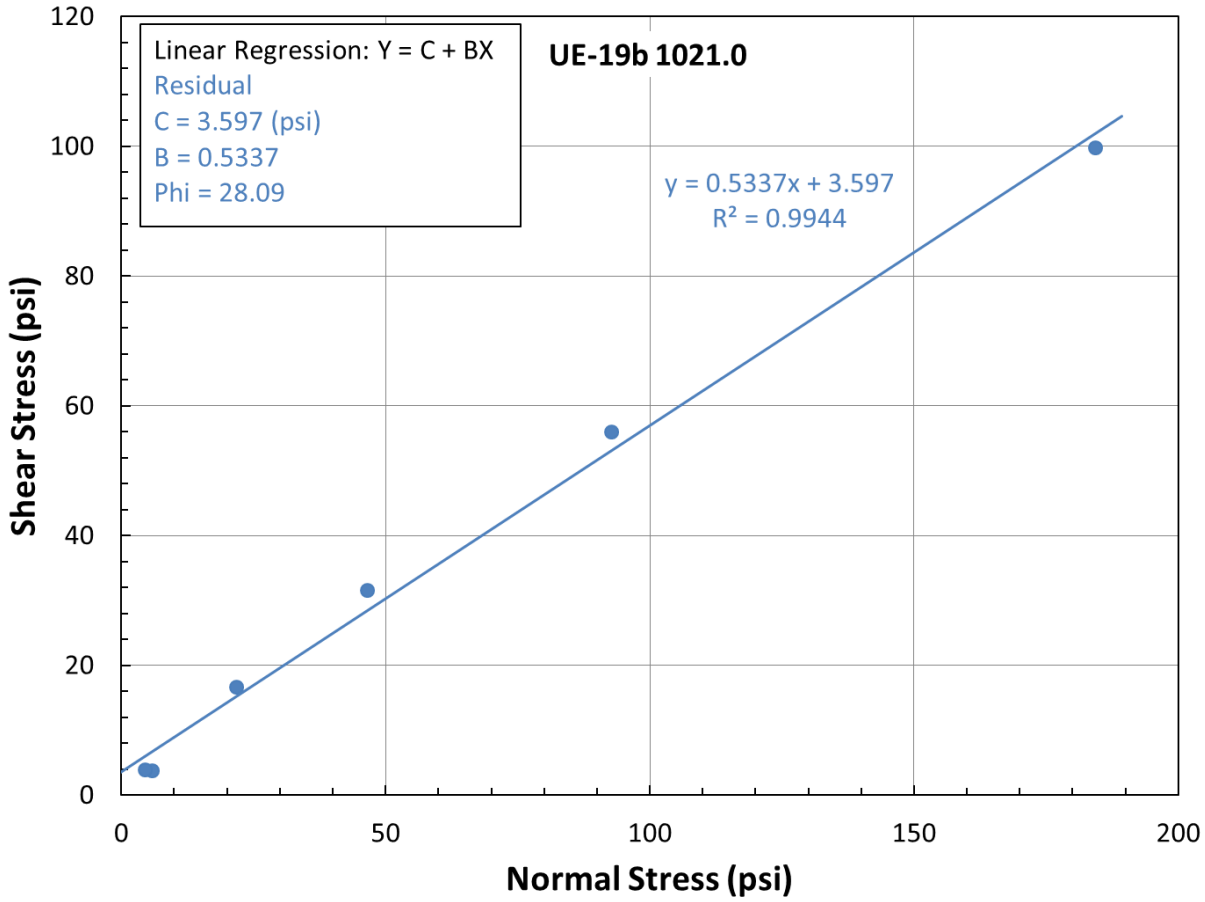

Figure 24. Shear stress versus Normal stress for UE-19b 1021.0

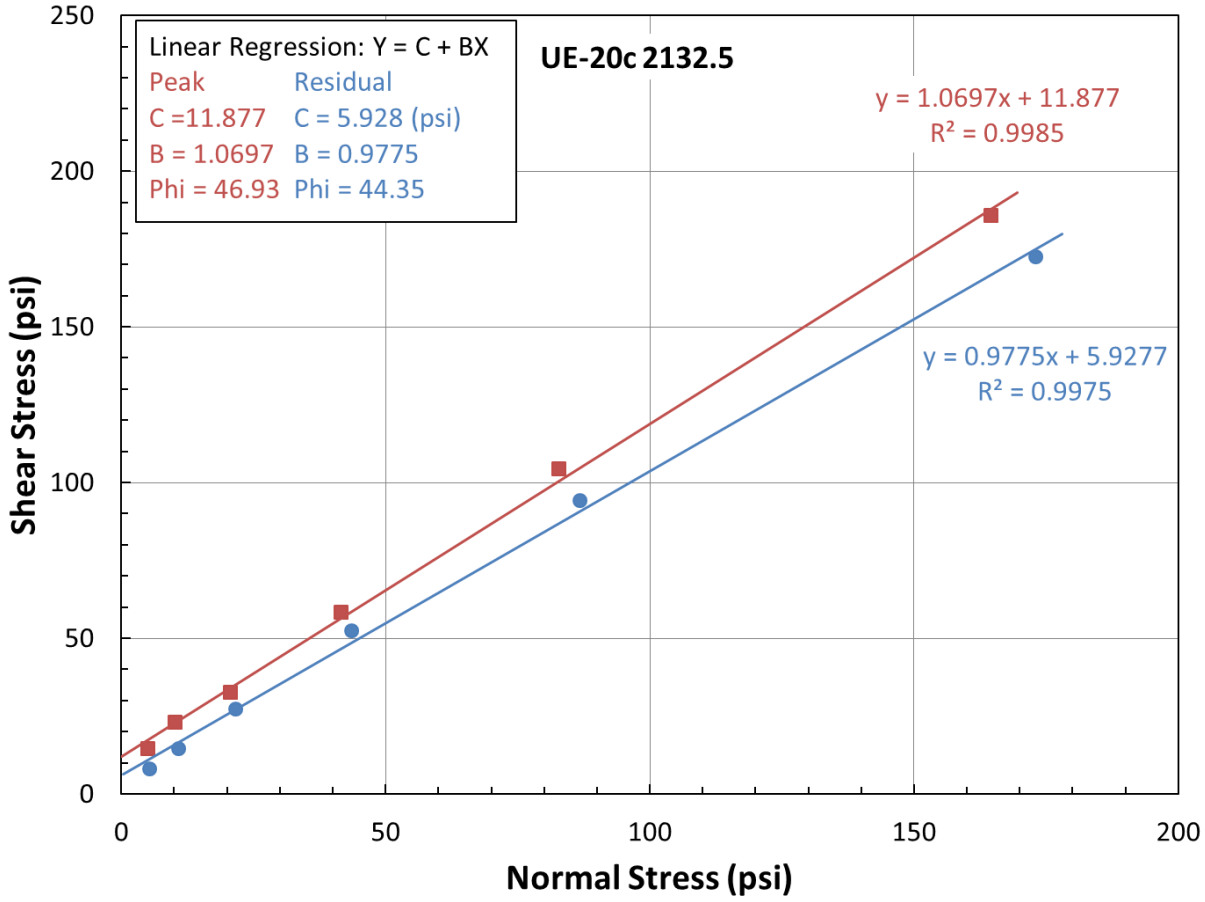

Figure 25. Shear stress versus Normal stress for UE-20c 2132.5

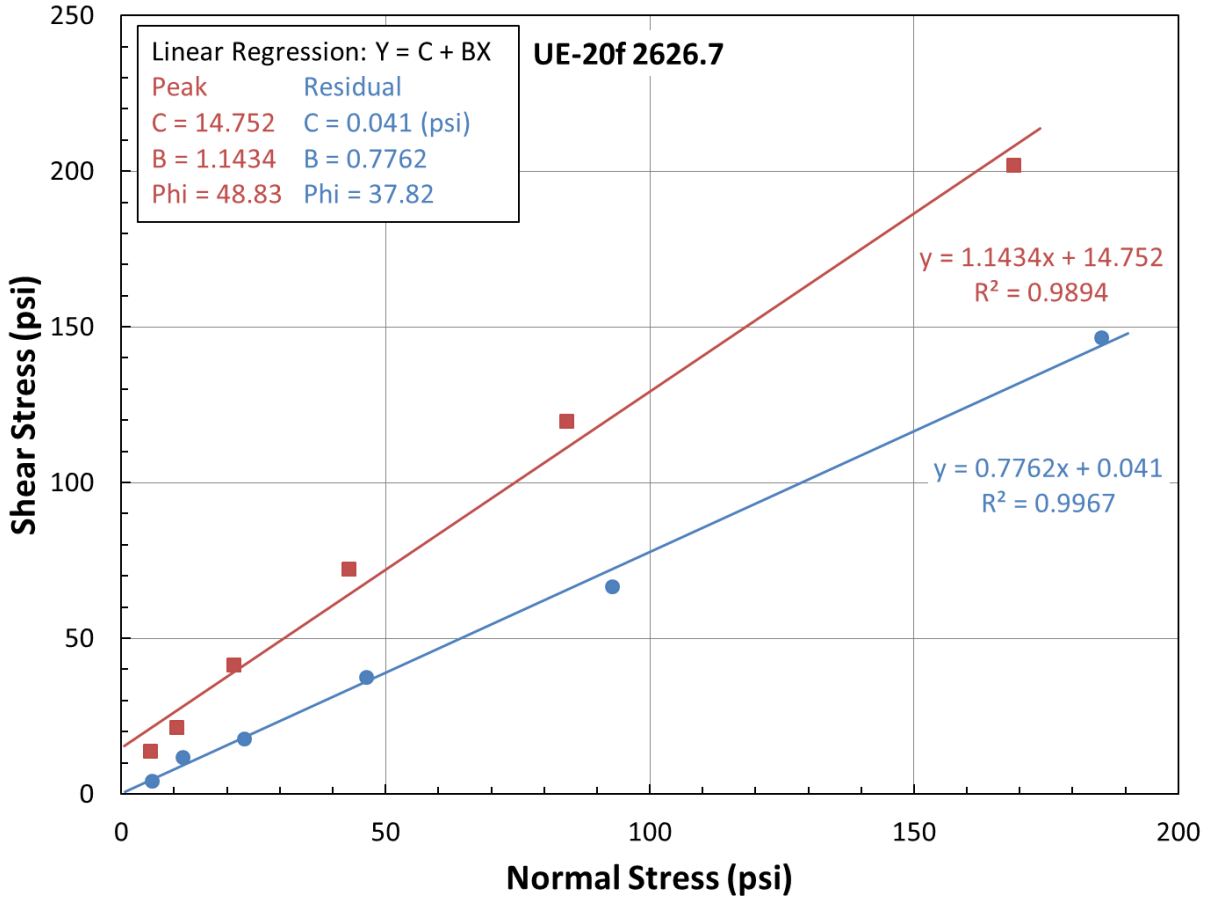

Figure 26. Shear stress versus Normal stress for UE-20f 2626.7

4. SUMMARY

A critical component of the Underground Nuclear Explosion Signatures Experiment (UNESE) program is a realistic understanding of the post-detonation processes and changes in the environment that produce observable physical and radio-chemical signatures. The comparison between a pre and post-detonation environment will be evaluated using theoretical and numerical models. A solid understanding of rock and fracture properties is needed to best model a UNESE test bed at any stage in its "life". To best support the need to accurately model UNE scenarios, an experimental program to determine the permeability and direct shear fractures properties of Barnwell core was developed. Gas permeability at varying confining pressure on nine samples and direct shear tests on two natural fractures and one fracture along a preexisting weakness plane were performed. Room temperature gas permeability measurements of Barnwell core dried at 50°C were found to yield permeability ranging from 6.24E-02 Darcys to 6.98E-08 Darcys. Friction angles from the direct shear tests vary from 28.1° to 44.4° for residual shear strength and average 47.9° for peak shear strength. Cohesion averaged 3.2 psi and 13.3 psi for residual and peak shear strength values respectively.

This page intentionally left blank.

APPENDIX A

FIGURES

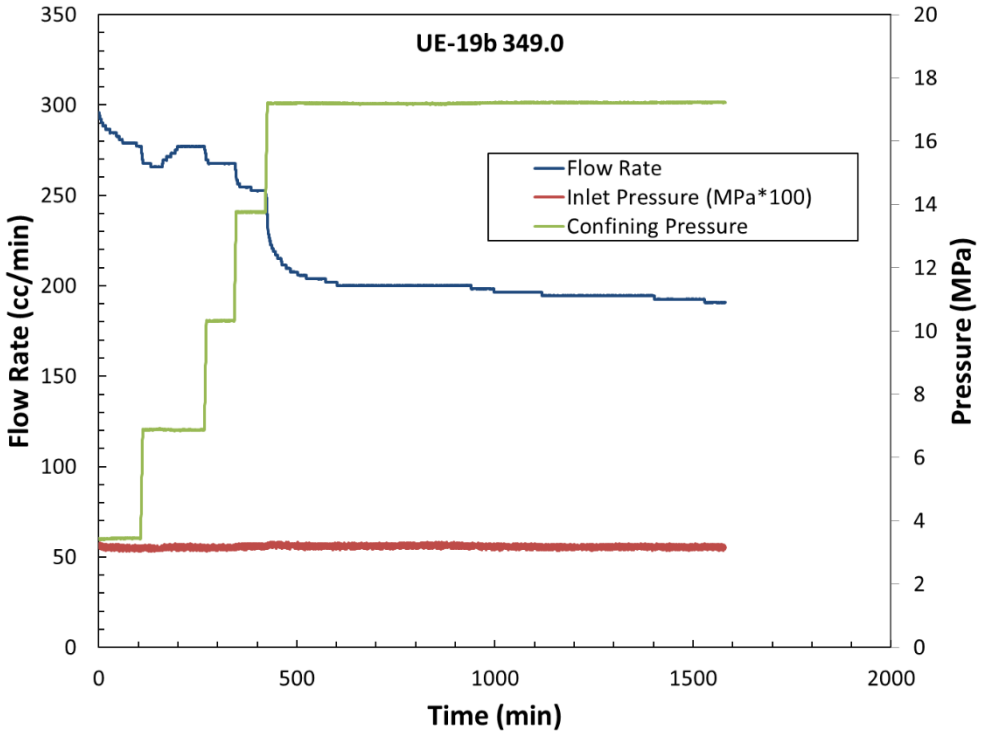

Figure A-1. Flow conditions (confining pressure, upstream pressure, and flow rate) versus time.

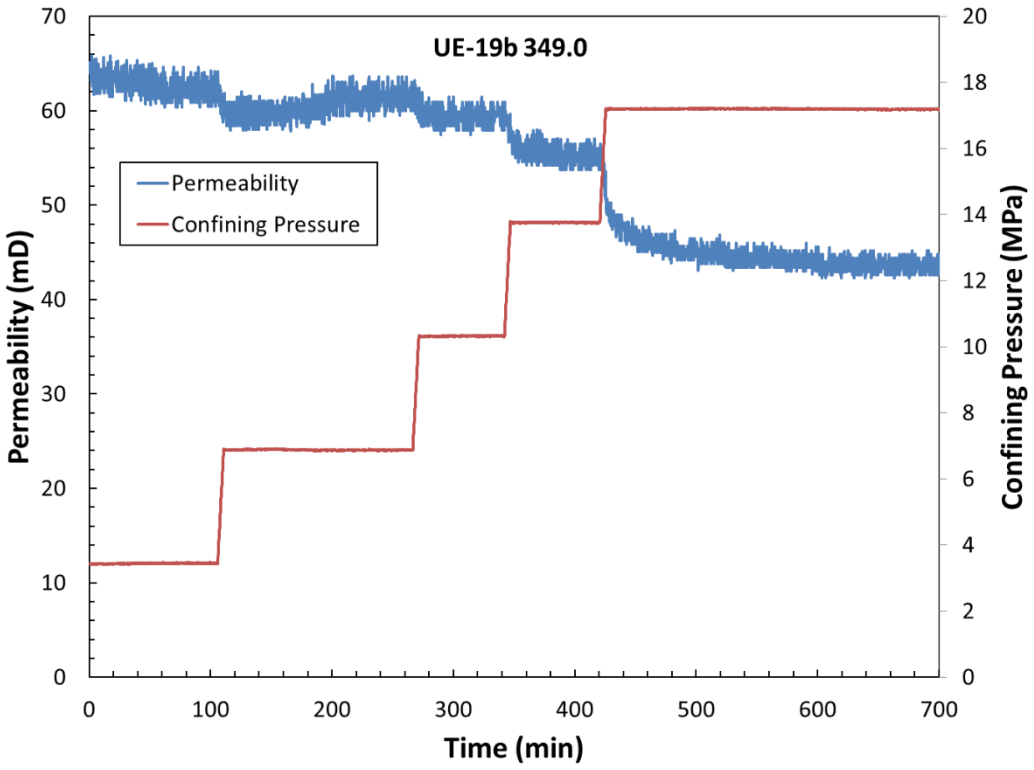

Figure A-2. Permeability and confining pressure versus time.

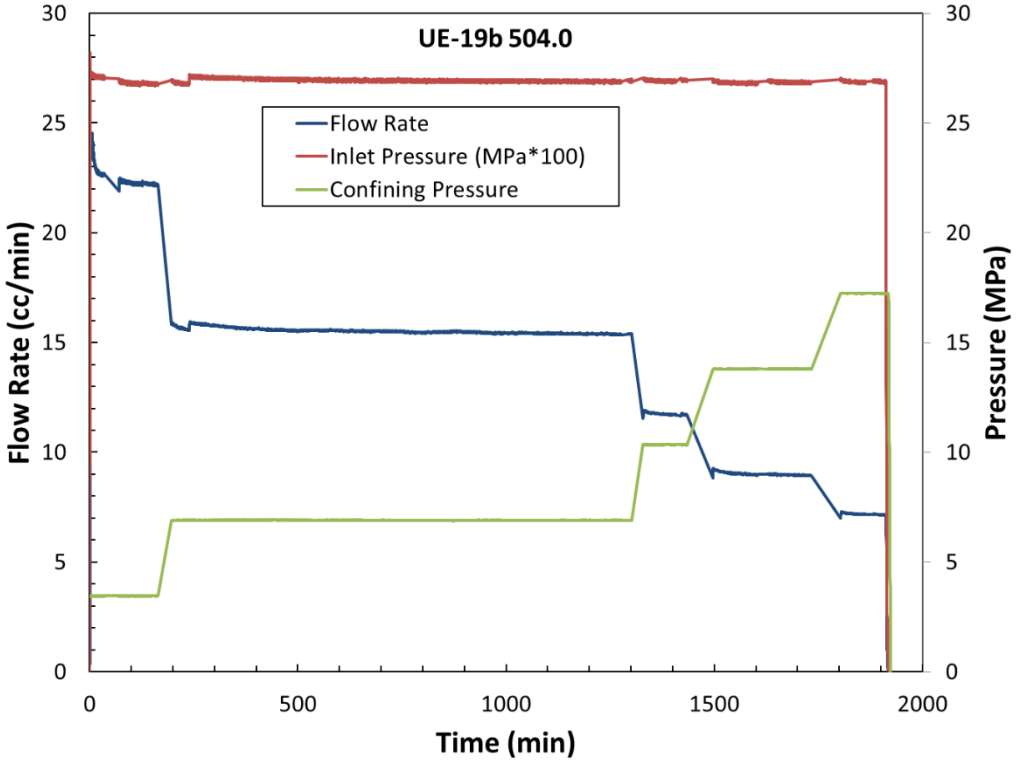

Figure A-3. Flow conditions (confining pressure, upstream pressure, and flow rate) versus time.

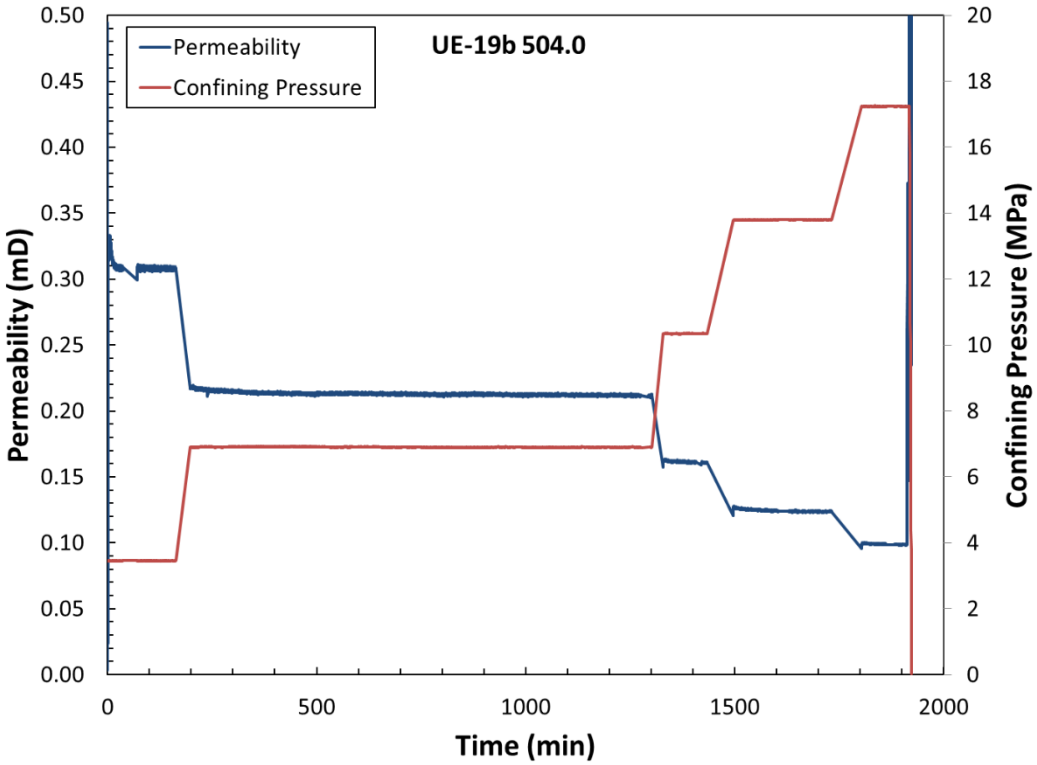

Figure A-4. Permeability and confining pressure versus time.

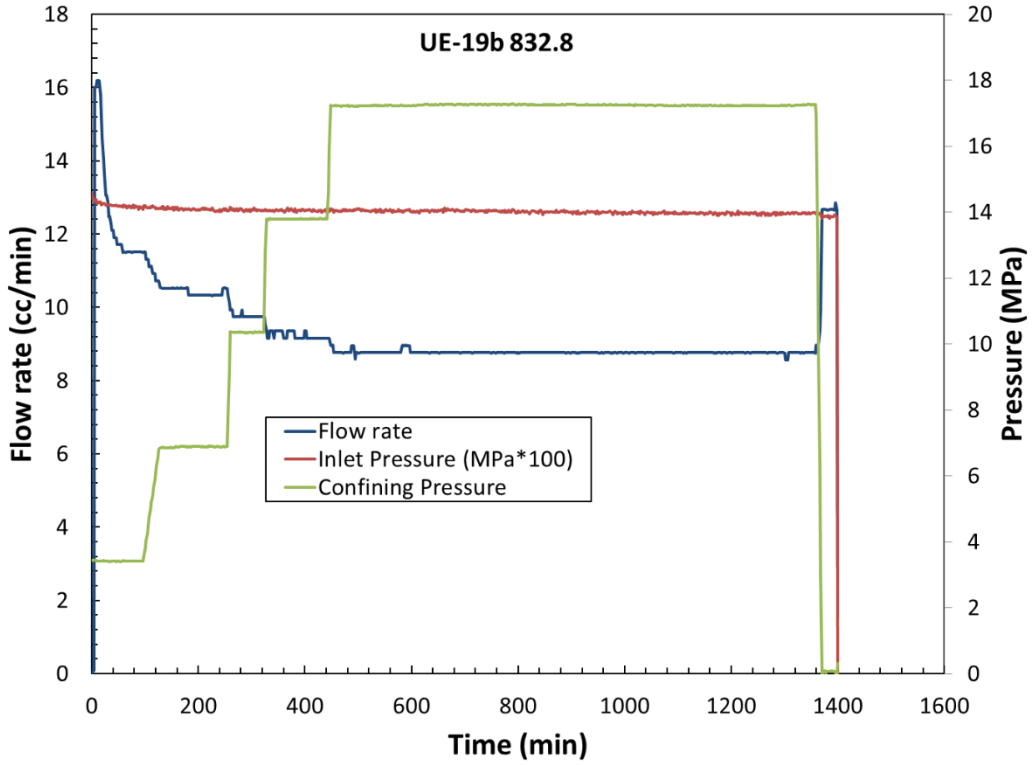

Figure A-5. Flow conditions (confining pressure, upstream pressure, and flow rate) versus time.

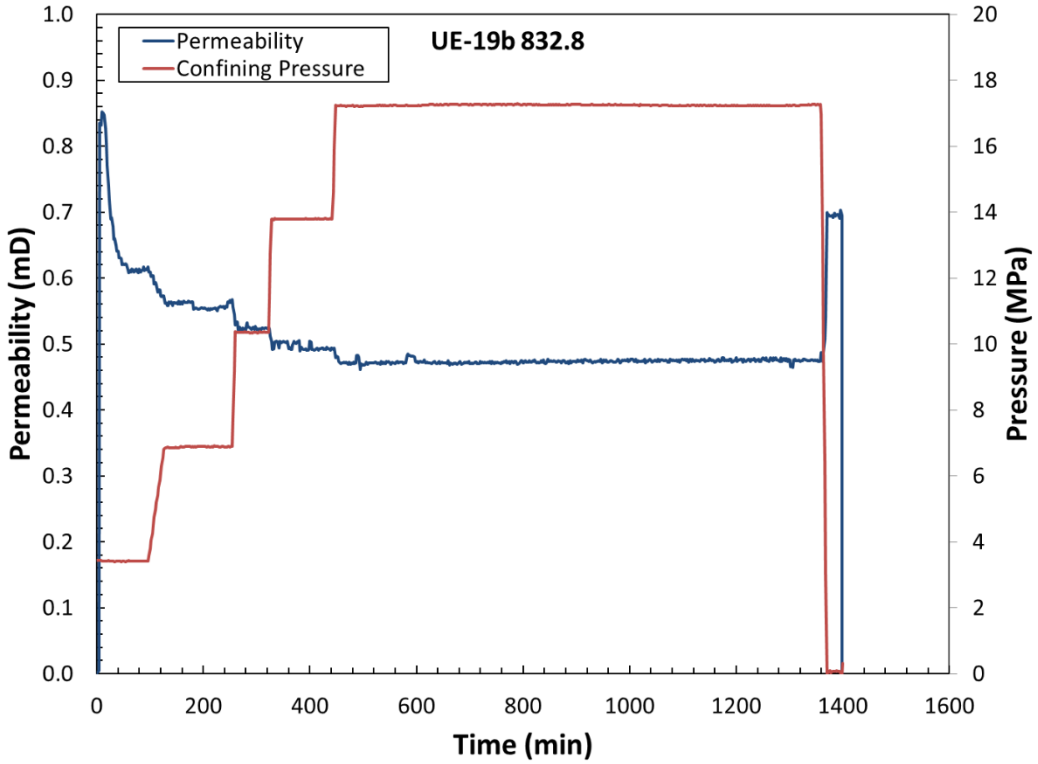

Figure A-6. Permeability and confining pressure versus time.

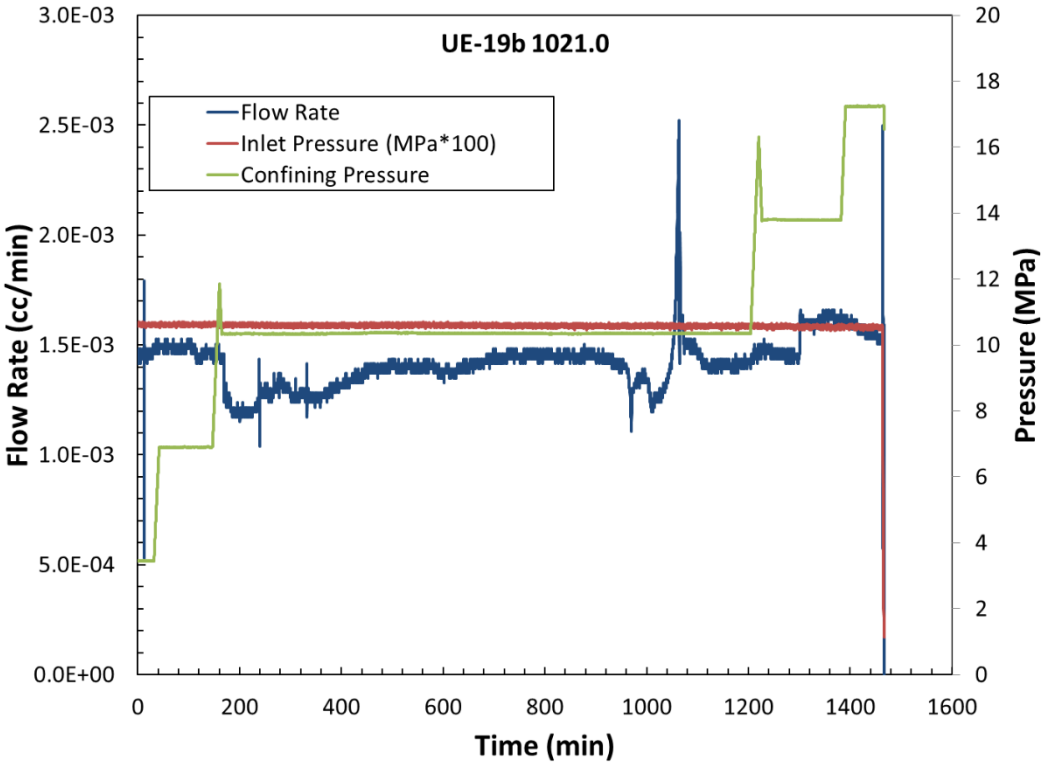

Figure A-7. Flow conditions (confining pressure, upstream pressure, and flow rate) versus time.

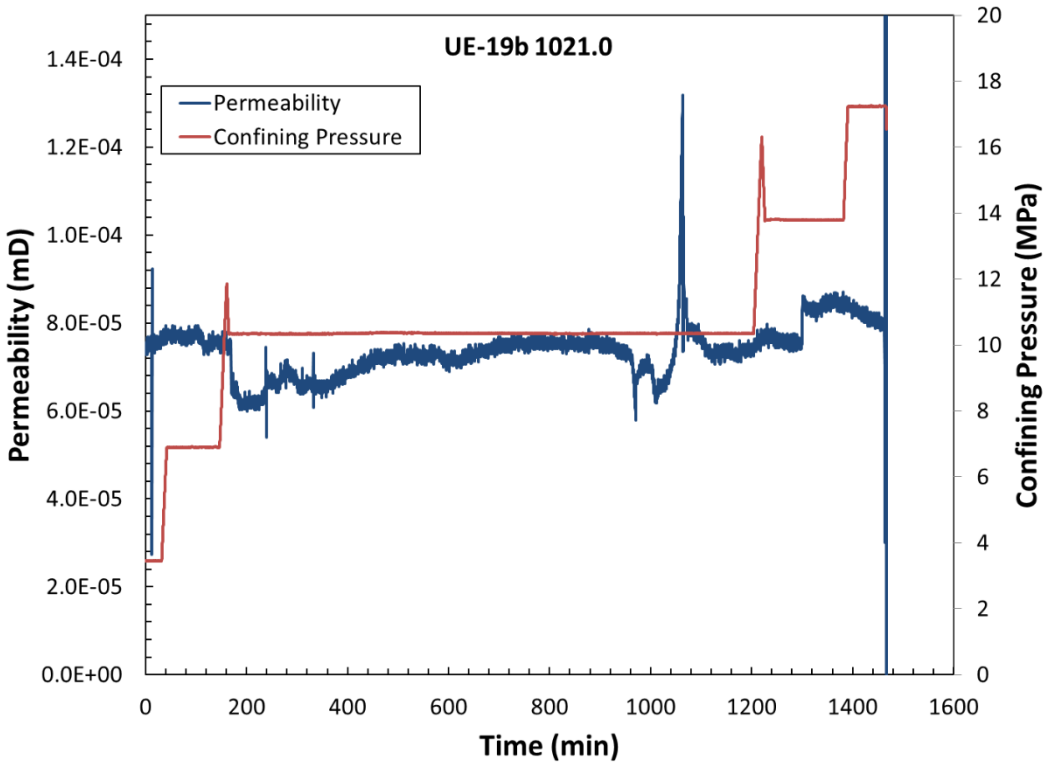

Figure A-8. Permeability and confining pressure versus time.

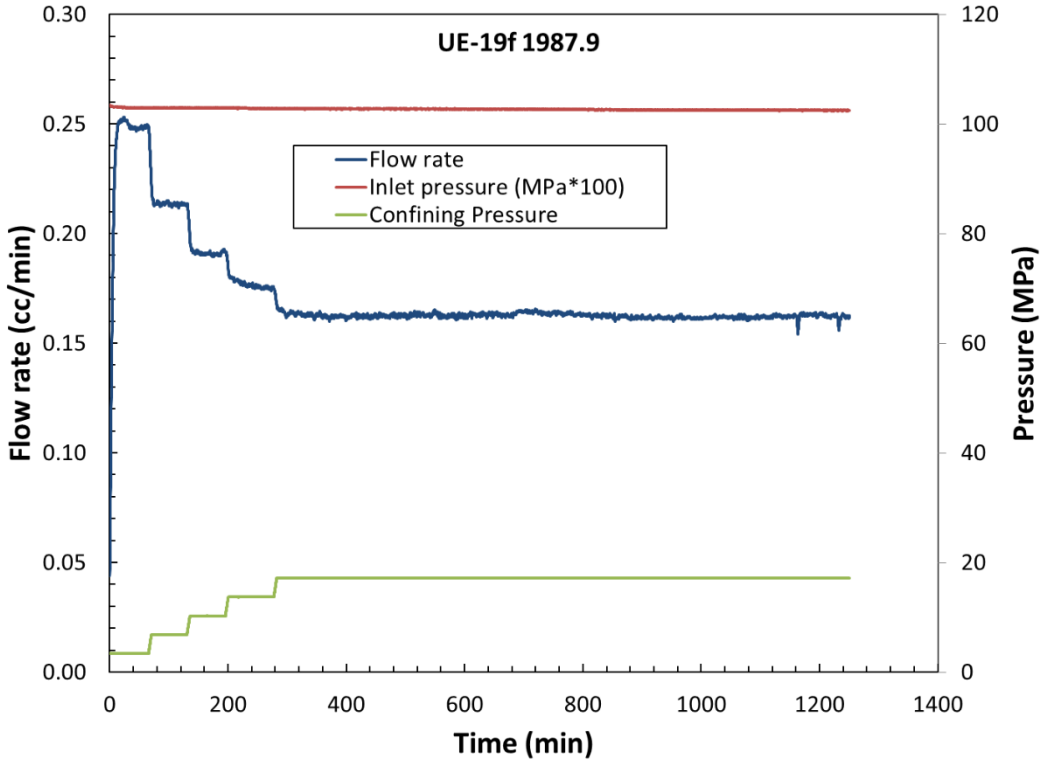

Figure A-9. Flow conditions (confining pressure, upstream pressure, and flow rate) versus time.

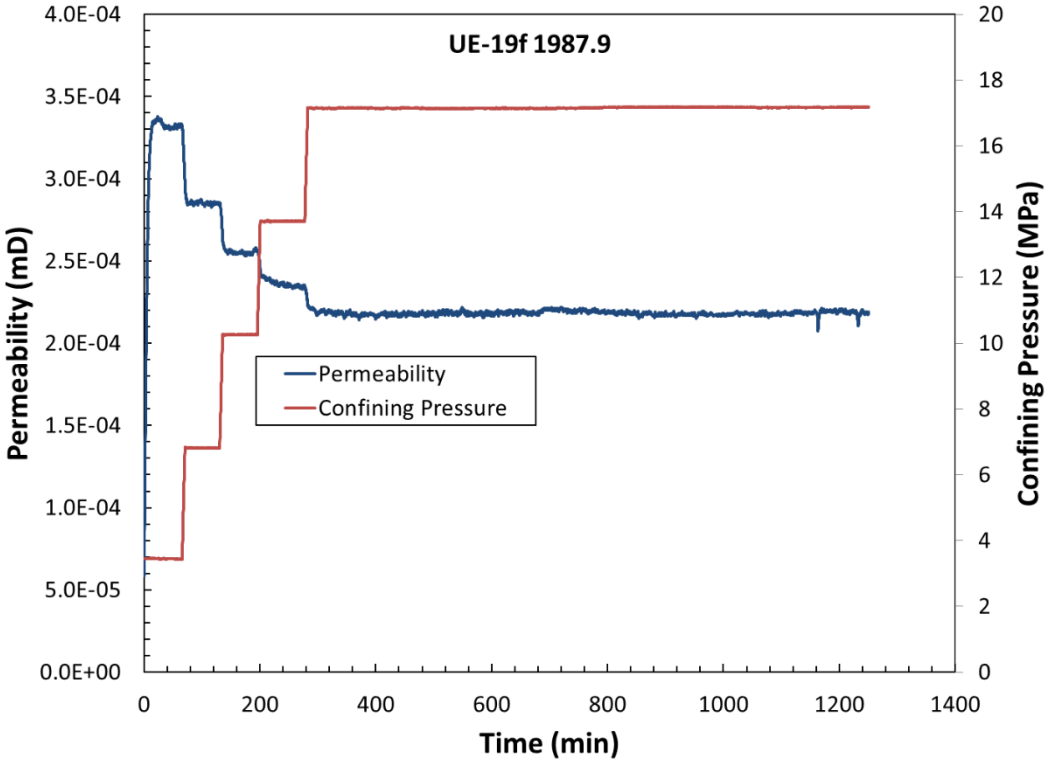

Figure A-10. Permeability and confining pressure versus time.

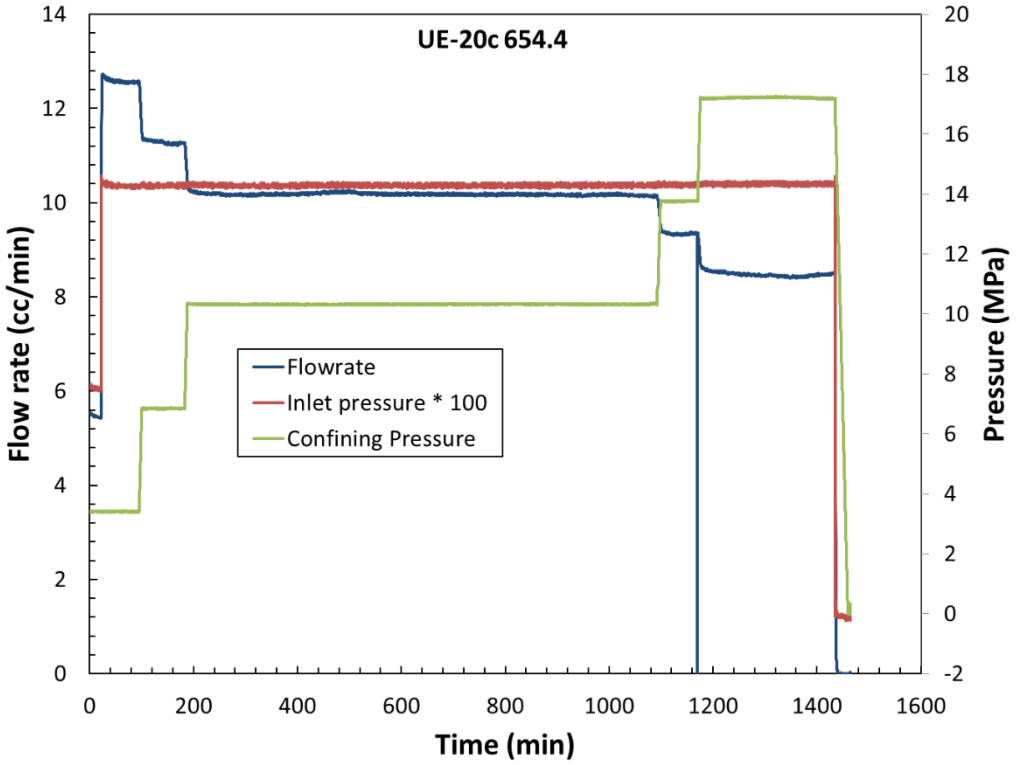

Figure A-11. Flow conditions (confining pressure, upstream pressure, and flow rate) versus time.

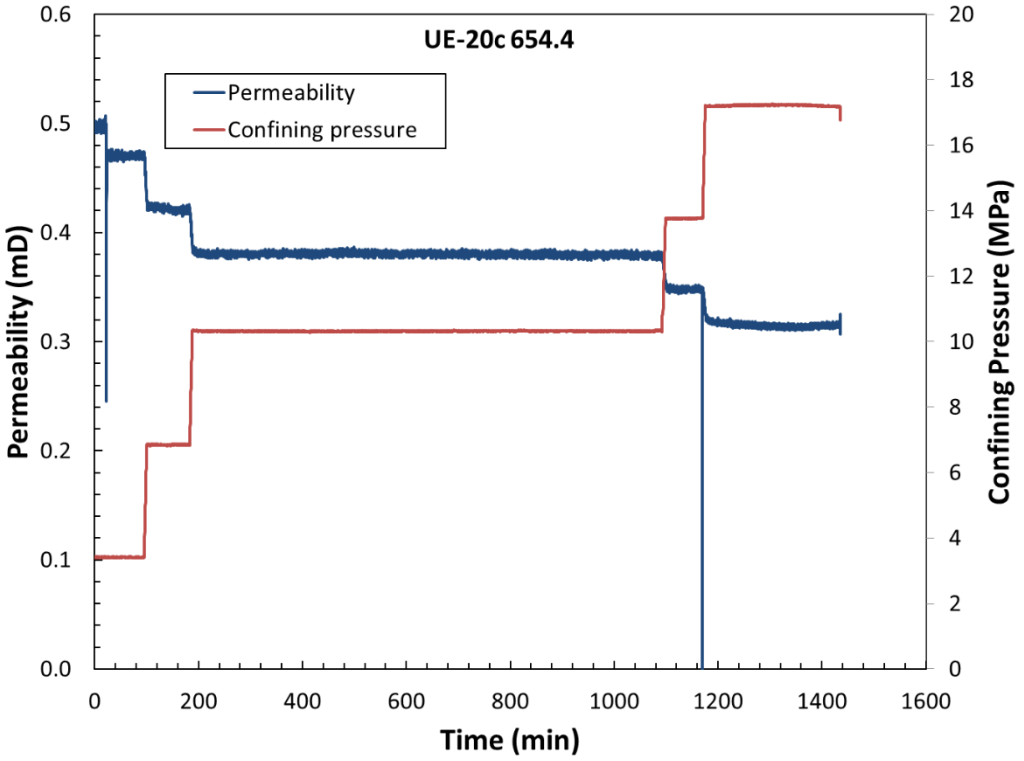

Figure A-12. Permeability and confining pressure versus time.

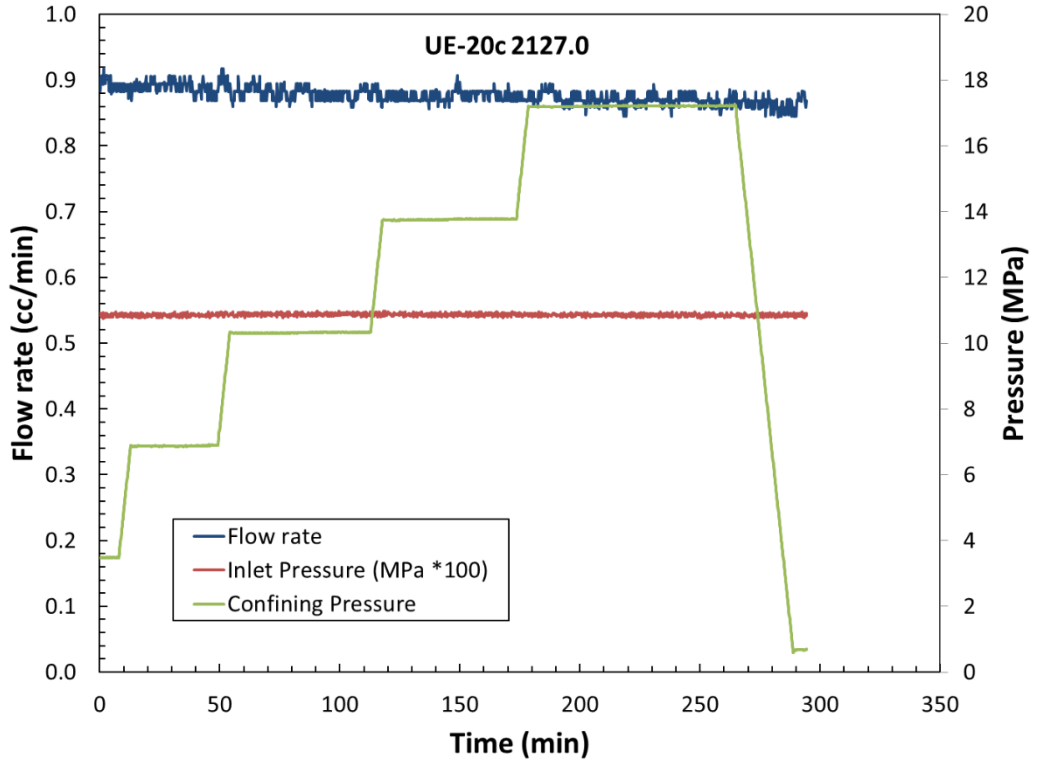

Figure A-13. Flow conditions (confining pressure, upstream pressure, and flow rate) versus time.

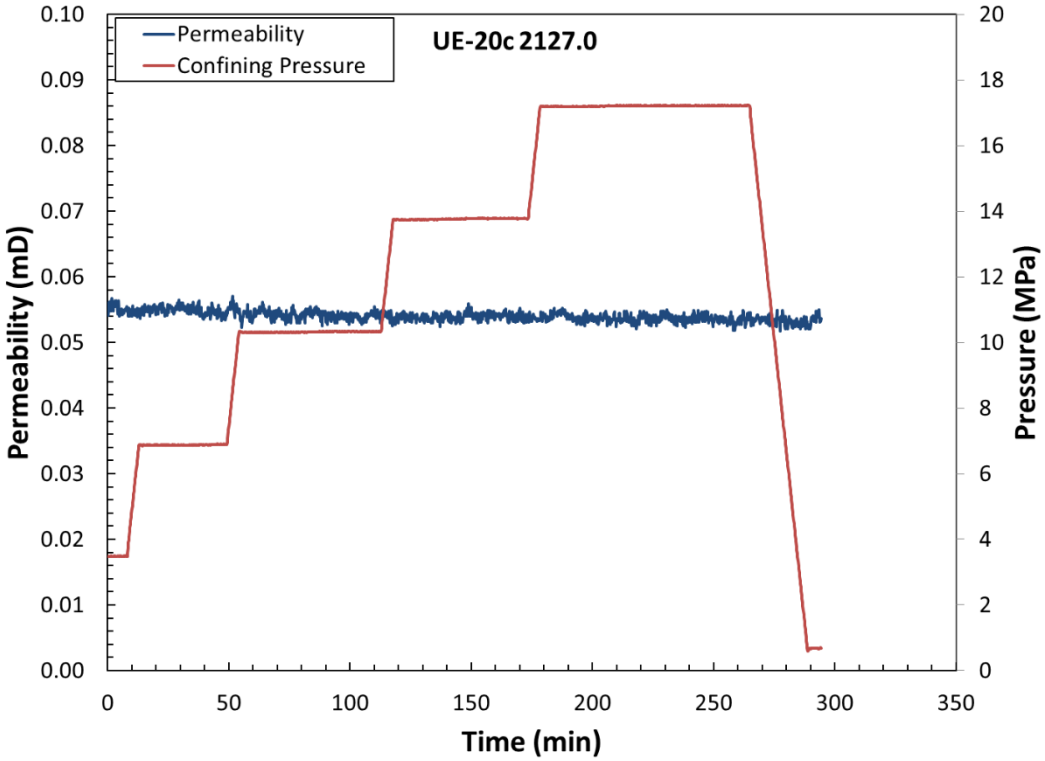

Figure A-14. Permeability and confining pressure versus time.

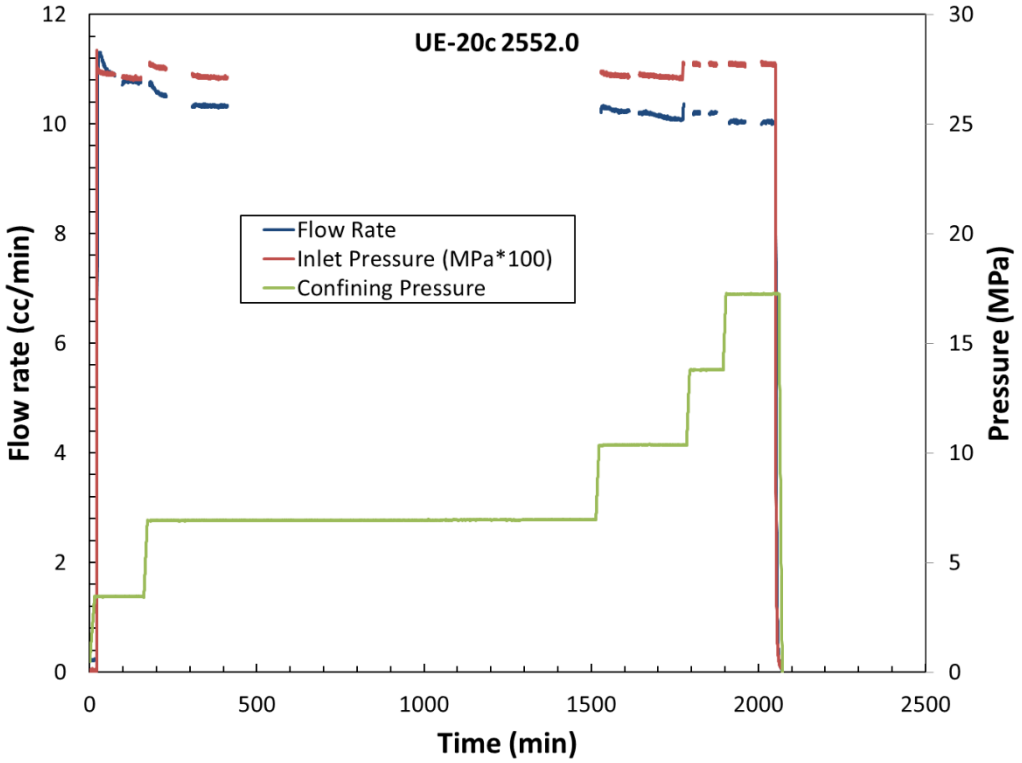

Figure A-15. Flow conditions (confining pressure, upstream pressure, and flow rate) versus time.

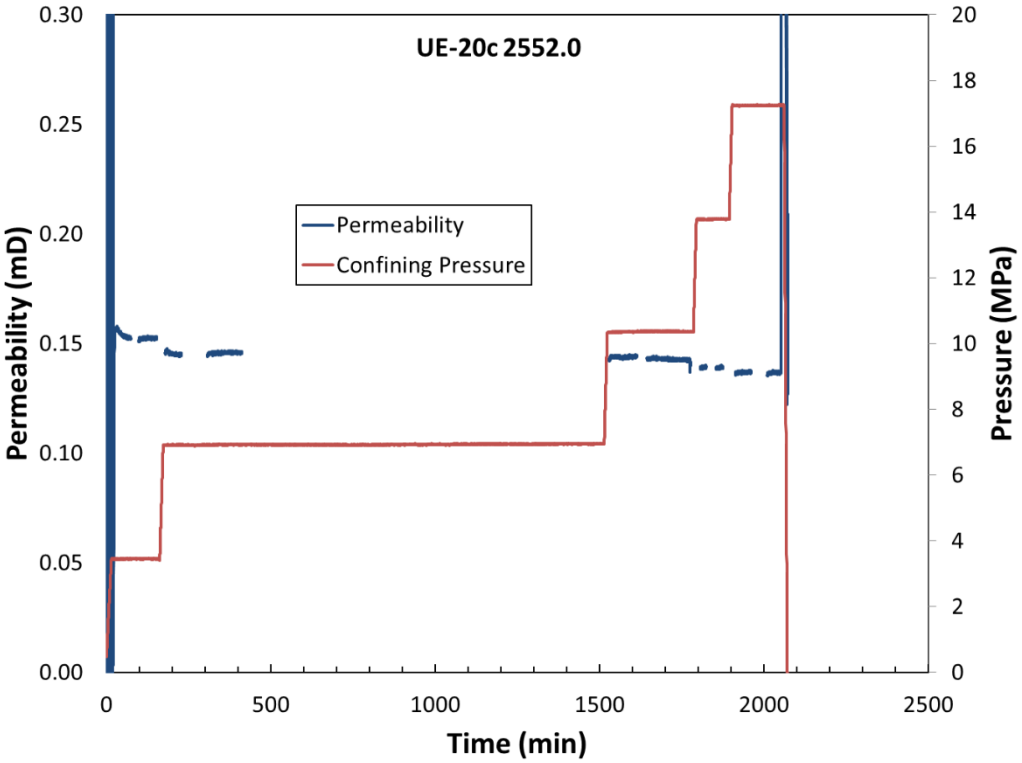

Figure A-16. Permeability and confining pressure versus time.

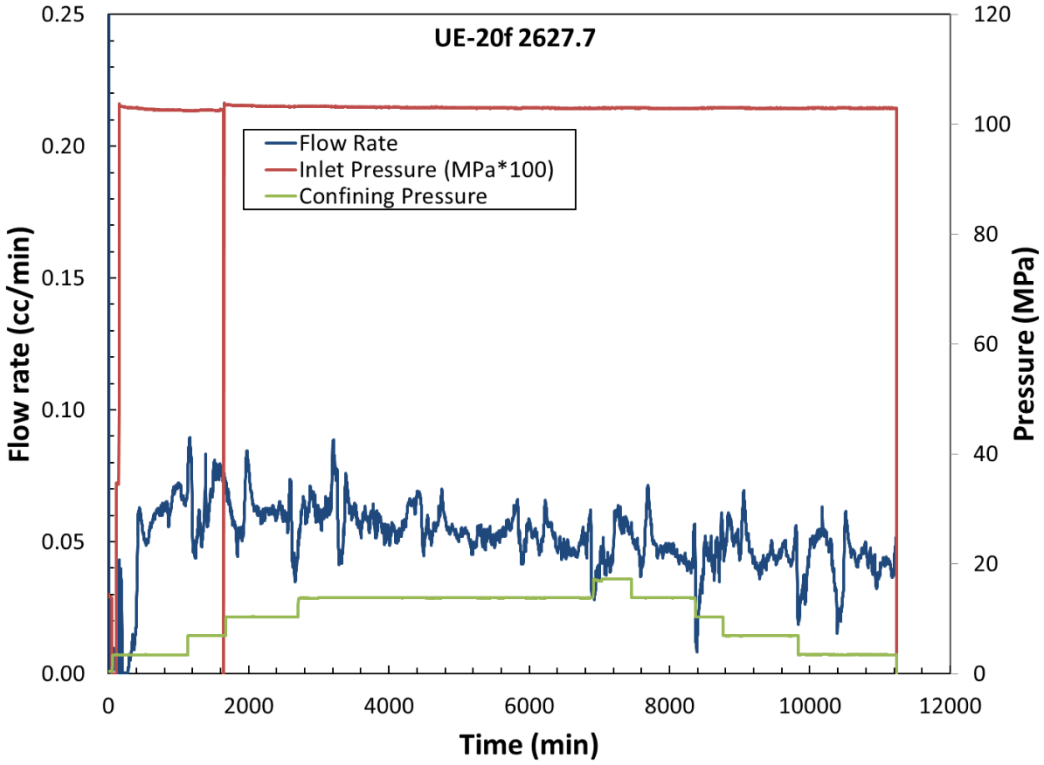

Figure A-17. Flow conditions (confining pressure, upstream pressure, and flow rate) versus time.

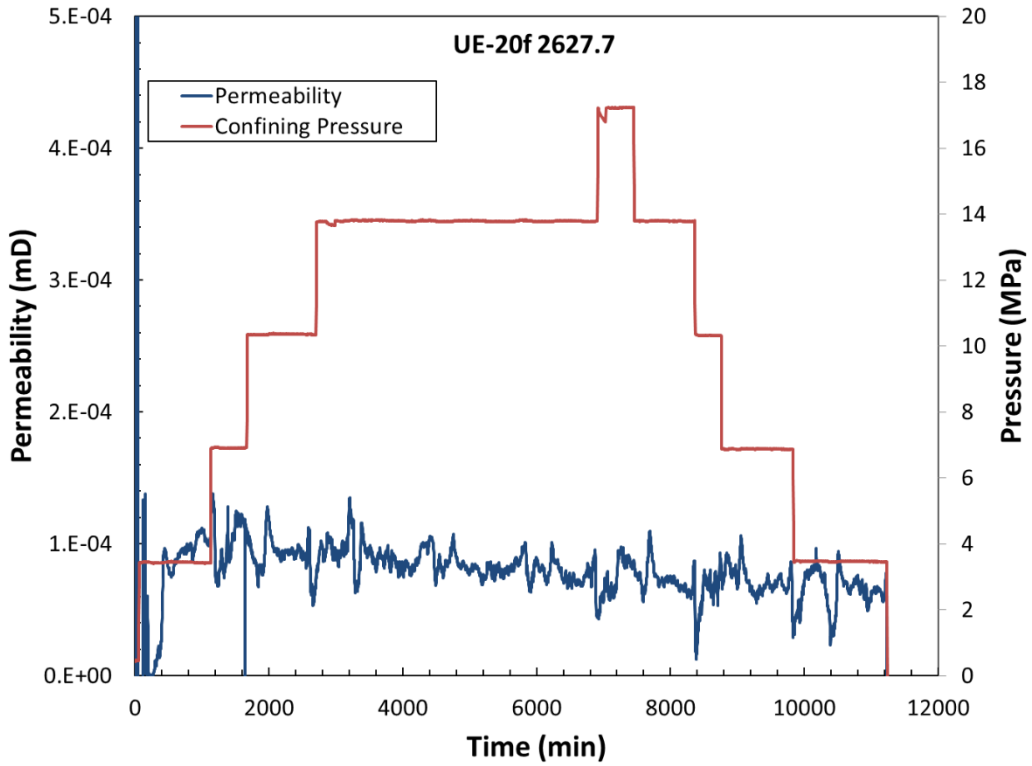

Figure A-18. Permeability and confining pressure versus time.

This page intentionally left blank.

DISTRIBUTION

1 MS-0899 Technical Library, 9536 (electronic copy)
1 MS-0899 RIM-Reports Management, 9532. (electronic copy)
1 MS-0612 Review & Approval Desk, 9612

Hard Copies:

Scott Broome (SNL)
Perry Parrow (SNL)

Electronic copies:

Moo Lee (SNL)
Steve Bauer (SNL)
Mathew Ingraham (SNL)


Sandia National Laboratories